Final Report *October 1975*

AIR MOTION DETERMINATION BY TRACKING HUMIDITY PATTERNS IN ISENTROPIC LAYERS

By: R. L. MANCUSO and D. J. HALL

Prepared for:

NATIONAL AERONAUTICS AND SPACE ADMINISTRATION
GODDARD SPACE FLIGHT CENTER
GREENBELT, MARYLAND 20771

CONTRACT NAS 5-20046

SRI Project 3320

STANFORD RESEARCH INSTITUTE
Menlo Park, California 94025 · U.S.A.

STANFORD RESEARCH INSTITUTE
Menlo Park, California 94025 • U.S.A.

Final Report *October 1975*

AIR MOTION DETERMINATION BY TRACKING HUMIDITY PATTERNS IN ISENTROPIC LAYERS

By: R. L. MANCUSO and D. J. HALL

Prepared for:

NATIONAL AERONAUTICS AND SPACE ADMINISTRATION
GODDARD SPACE FLIGHT CENTER
GREENBELT, MARYLAND 20771

Attention: JAMES R. GREAVES

CONTRACT NAS 5-20046

SRI Project 3320

Approved by.

R T. H. COLLIS, *Director*
Atmospheric Sciences Laboratory

RAY L. LEADABRAND, *Executive Director*
Electronics and Radio Sciences Division

ABSTRACT

Investigations were carried out on determining air motions by tracking humidity patterns in isentropic layers. Upper-air rawinsonde data from the NSSL network and from the AVE-II pilot experiment were used to simulate temperature and humidity profile data that will eventually be available from geosynchronous satellites. Polynomial surfaces that move with time were fitted to the mixing-ratio values of the different isentropic layers. The velocity components of the polynomial surfaces are part of the coefficients that are determined in order to give an optimum fitting of the data. In the mid-troposphere, the derived humidity motions were in good agreement with the winds measured by rawinsondes so long as there were few or no clouds and the lapse rate was relatively stable. In the lower troposphere, the humidity motions were unreliable primarily because of non-adiabatic processes and unstable lapse rates. In the upper troposphere, the humidity amounts were too low to be measured with sufficient accuracy to give reliable results. However, it appears that humidity motions could be used to provide mid-tropospheric wind data over large regions of the globe. Verification of these results using satellite data should be possible in the near future.

Investigations were also carried out to determine the feasibility of using the ISODATA dynamic clustering technique for tracking regions of high or low humidity in isentropic layers. Statistically simulated humidity fields were used since actual satellite data were not available. In these simulations, clusters were generated to give a representation similar to an actual THIR 6.7 μm image of humidity patterns. Fields two hours ahead and behind were also generated using arbitrarily assigned cluster motions. The ISODATA program was then used to identify and

determine the motions of the clusters. In situations where the cluster patterns are reasonably distinguishable by eye, good results were obtained. However, where clusters are complex and difficult to identify, a few bad motion measurements can occur that increase the rms error considerably. Consequently, some type of screening, either by the human eye or by computer, is required to keep the rms errors reduced to an acceptable level. With this addition, the ISODATA clustering technique appears to provide a suitable tracking approach for use in routine applications, and it is relatively efficient.

CONTENTS

ILLUSTRATIONS

ACKNOWLEDGEMENTS

This study was supported by the National Aeronautics and Space Administration under Contract NAS 5-20046.

The authors wish to acknowledge the help of Dr. Paul A. Davis for his many discussions and ideas. Also, Mr. Dan E. Wolf provided very capable support in adapting the ISODATA computer program for use in tracking humidity fields.

I INTRODUCTION

Cloud motions shown by sequences of pictures from geostationary satellites provide excellent estimates of the winds if the cloud heights are known and proper interpretations are made (Davis et al., 1973; Fujita et al., 1975). However, in large regions of the globe, the atmosphere is relatively cloud-free or contains primarily low clouds. Thus, a method for determining winds in cloud-free regions is needed, particularly in the tropics where the geostrophic relationship is of limited use (Endlich and Mancuso, 1972). The determination of air motion in such regions may be possible by tracking humidity motions on isentropic surfaces as proposed by Endlich, Mancuso, and Nagle (1972). The basic data needed are measurements of vertical profiles of temperature and humidity from geosynchronous satellites that can be used to generate time sequences of the mixing ratios on isentropic surfaces. If the method proves feasible, such humidity motions in cloud-free regions would be a very valuable source of wind data, since lack of an accurate initial analysis is still one of the major sources of error in numerical weather prediction (Haltiner and Williams, 1975).

The study described in this report investigated the possibility of determining air motions in this manner. The work was carried out under Contract NAS 5-20046 for the National Aeronautics and Space Administration at Goddard Space Flight Center. In Section II, the basic concept is tested by comparing humidity motions in an isentropic layer with the actual winds--rawinsonde observations were used since actual satellite data are not yet available. In Section III, the feasibility of real-time automated tracking of the motions of humidity packets (regions of high or low humidity) is considered using simulated humidity fields.

II HUMIDITY MOTIONS IN ISENTROPIC LAYERS

A. Basic Concept

Satellite measurements of radiances in a number of narrow spectral intervals provide a remote measurement of atmospheric temperature as a function of pressure (Wark and Fleming, 1966). Additional radiances measured in the water-vapor rotation band can be used for obtaining vertical profiles of humidity (Conrath et al., 1970; Smith and Howell, 1971). Improvements of the satellite sensors and of mathematical techniques for deriving vertical temperature and humidity profiles are continuously being made (Blackmer et al., 1974). Thus, reliable profile data should eventually be available for most portions of the atmosphere that can be sensed from geosynchronous satellites. The regions of the atmosphere that cannot be probed in this indirect manner are layers of dense cloud, the atmosphere beneath them, and regions lying outside the satellite's field of view.

These measurements of temperature and water vapor profiles are weighted average values for up to about seven vertical layers. They represent the general atmospheric structure accurately for global analysis, but do not reveal the presence of detailed features, such as temperature inversions or jet streaks (Togstad and Horn, 1974). The data may be processed directly to give values of potential temperature and mixing ratio versus pressure. Also, thickness values between pressure surfaces, such as the stability parameter $\partial\theta/\partial p$, can be computed. Therefore, analyses of pressure, mixing ratio, and stability on selected isentropic surfaces (or layers) can be made for the areas viewed at intervals given by the cycling time of the satellite's scanning pattern, which is approximately one hour.

For dry adiabatic processes, the mixing ratio (m) is conserved on a potential temperature (θ) surface; that is, mixing-ratio patterns move with the wind (Rossby and collaborators, 1937). Thus, using time sequences of isentropic mixing-ratio patterns, it should be possible to track the patterns in a manner analogous to the present tracking of clouds from sequences of cloud pictures. Ideally, the motions of unsaturated humidity patterns would be complete wind vectors that include the divergent wind components. The major problems associated with isentropic analysis have been with the: (1) steep slopes of the isentropic surfaces and their intersection with the ground, and (2) the occurrence of superadiabatic lapse rates. These problems have been discussed in detail by Bleck (1973).

B. Approach and Data Used

To test the concept of determining winds by tracking humidity motions on isentropic surfaces, rawinsonde data were used as a substitute for actual satellite soundings, since the latter are not yet available. Conventional rawinsonde reports were not satisfactory due to the long interval (12 hours) between observations. Thus, data from special upper-air observational programs were used; that is, data from the NSSL rawinsonde network and the AVE-II experiment.

- NSSL--Special upper-air observations have been carried out by NSSL since 1966. Their upper-air mesonetwork for 1966 and 1967 is shown in Figure 1; soundings were generally made to 100 mb and at 90-minute intervals during periods of expected severe weather. Data for these years were obtained from NSSL (Barnes et al., 1971) and edited data for selected storms from the University of Missouri (Kung and McInnis, 1969). The NSSL data for later years (1968 and 1969) were not suitable for this study. The stations were spaced much closer together and the soundings only reached to about 500 mb. Also, there were relatively few successive times at which soundings were made for each

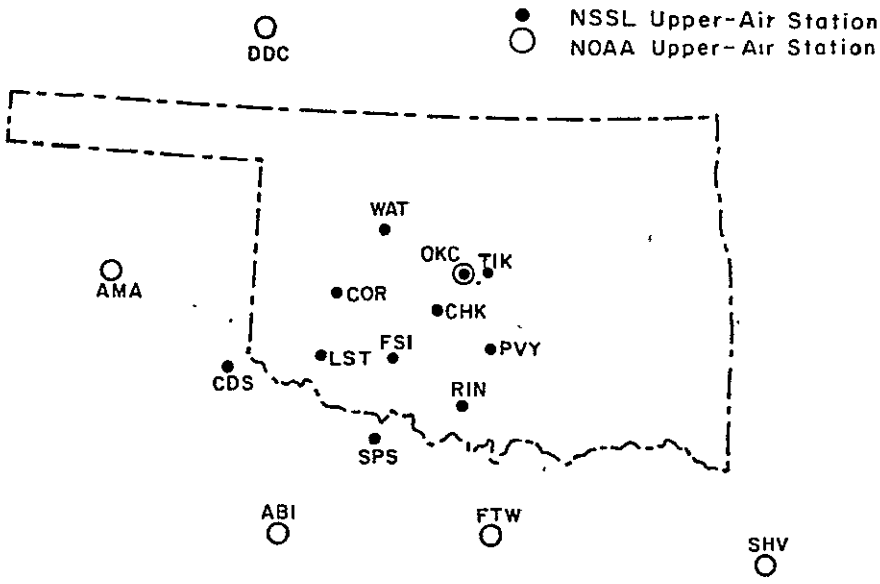

FIGURE 1 NSSL MESOSCALE RAWINSONDE NETWORK FOR 1966 AND 1967

case. In the 1966-67 years, there were generally four or five successive times at which soundings were made, thus, permitting a best fitting of the data.

- AVE-II--An upper-air experiment was carried out by NASA over a 24-hour period (1200 GMT 11 May to 1200 GMT 12 May 1974). During this experiment, 54 of the standard U.S. upper-air reporting stations made special soundings up to 25 mb at 3-hourly intervals; these stations are shown in Figure 2. Data from this experiment were made available by Scoggins and Turner (1974) and Fuelberg (1974).

The AVE-II experiment gives data spaced about 200 miles apart and this would be consistent with the sounding capabilities of current satellite systems. The NSSL data are spaced about 50 miles apart and permit depiction of mesoscale features; future satellite systems may possibly be able to provide this density of soundings. Both the NSSL and AVE-II rawinsonde data give vertical resolutions considerably higher than do satellite soundings--which are currently limited to distinguishing between about seven or less vertical layers.

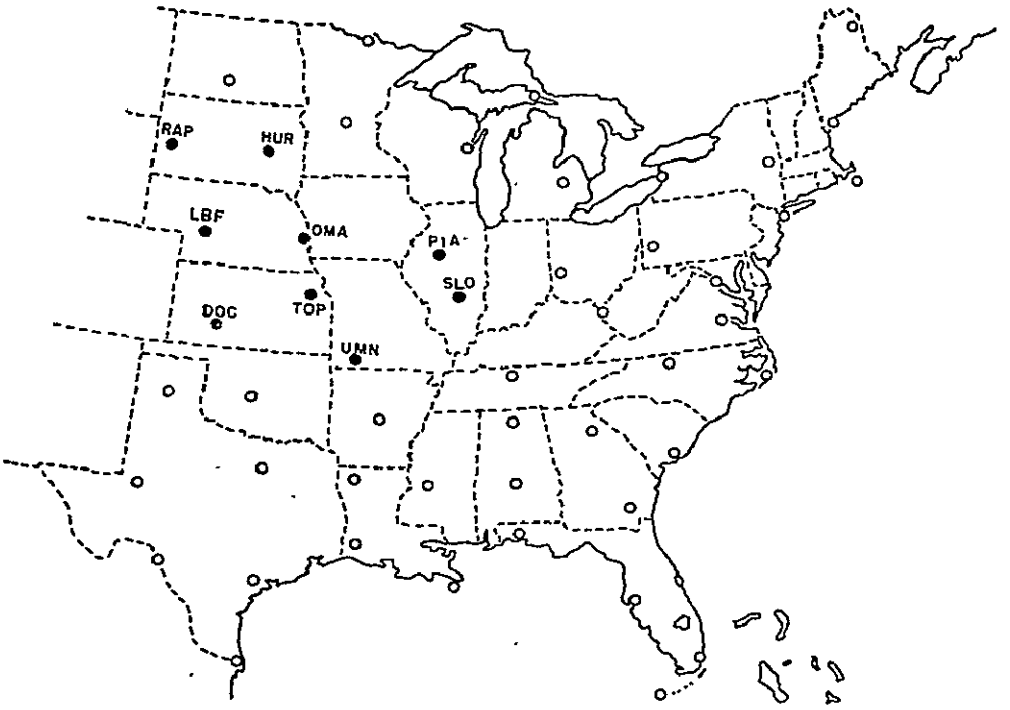

FIGURE 2 RAWINSONDE NETWORK FOR THE AVE-II EXPERIMENT
Solid circles denote the nine stations that were used in this study.

C. Error Considerations

Errors of rawinsonde observations have been discussed by various authors (e.g., Danielsen, 1959; Barnes et al., 1971; Scoggins and Turner, 1974; Brousaides, 1975). The error of the temperature sensing element is less than 1/2°C; however, a more reasonable estimate of the actual measurement error would be about 1°C. The error of relative humidity is less than 10 percent, but humidity measurements become unreliable when temperatures go below -20°C or when the relative humidity goes below 20 percent. The humidity hygristor element has also had a diurnal error due to heating by solar radiation, which has been corrected in the radiosonde instruments after about 1972 (Ruprecht, 1975). This error will

normally produce a difference of about 10 percent in the relative humidity values and will increase with height and clear skies. Although the NSSL soundings were subject to this diurnal error, it should be small relative to the horizontal variations in the data.

More significant is the relatively strong drop-off of mixing ratio with height, such as from 10 g/kg at 900 mb to 0.01 g/kg at 300 mb. Due to this, a small error in temperature or potential temperature can effectively produce a fairly large error in the mixing-ratio value. Figure 3 shows the θ versus m profile (solid line) for the NSSL station at Fort Sill (FSI) at 1354 CST, 22 May 1966. A noticeable increase in mixing ratio with height takes place near $\theta = 317^{\circ}$. Also, shown in Figure 3 are the profiles (dashed lines) that would result if the temperature were either $\pm 1^{\circ}$C in error (this neglects possible pressure and mixing-ratio errors). The possible range of mixing-ratio values that could be associated with a given θ surface is quite large (0.5 to 1.3 g/kg on the $\theta = 320^{\circ}$ surface), and comparable to the actual horizontal variations over the NSSL area (0.2 to 1.3 g/kg on the $\theta = 320^{\circ}$ surface). This problem may not be as important when actual satellite sounding data are used; since satellites should be able to provide relatively accurate measurements of the horizontal gradients of mixing ratio even though the absolute error may not be negligible. However, it would still appear desirable to use some measurement of humidity other than mixing ratio that would retain the same magnitude with height as does relative humidity.

Rawinsonde wind errors generally vary between about 1/2 to 5 m s^{-1} depending on the height and geometry involved; the greater the height and lower the elevation angle, the larger the error. In this study, the winds were generally not very strong and the wind errors should be near the lower value quoted.

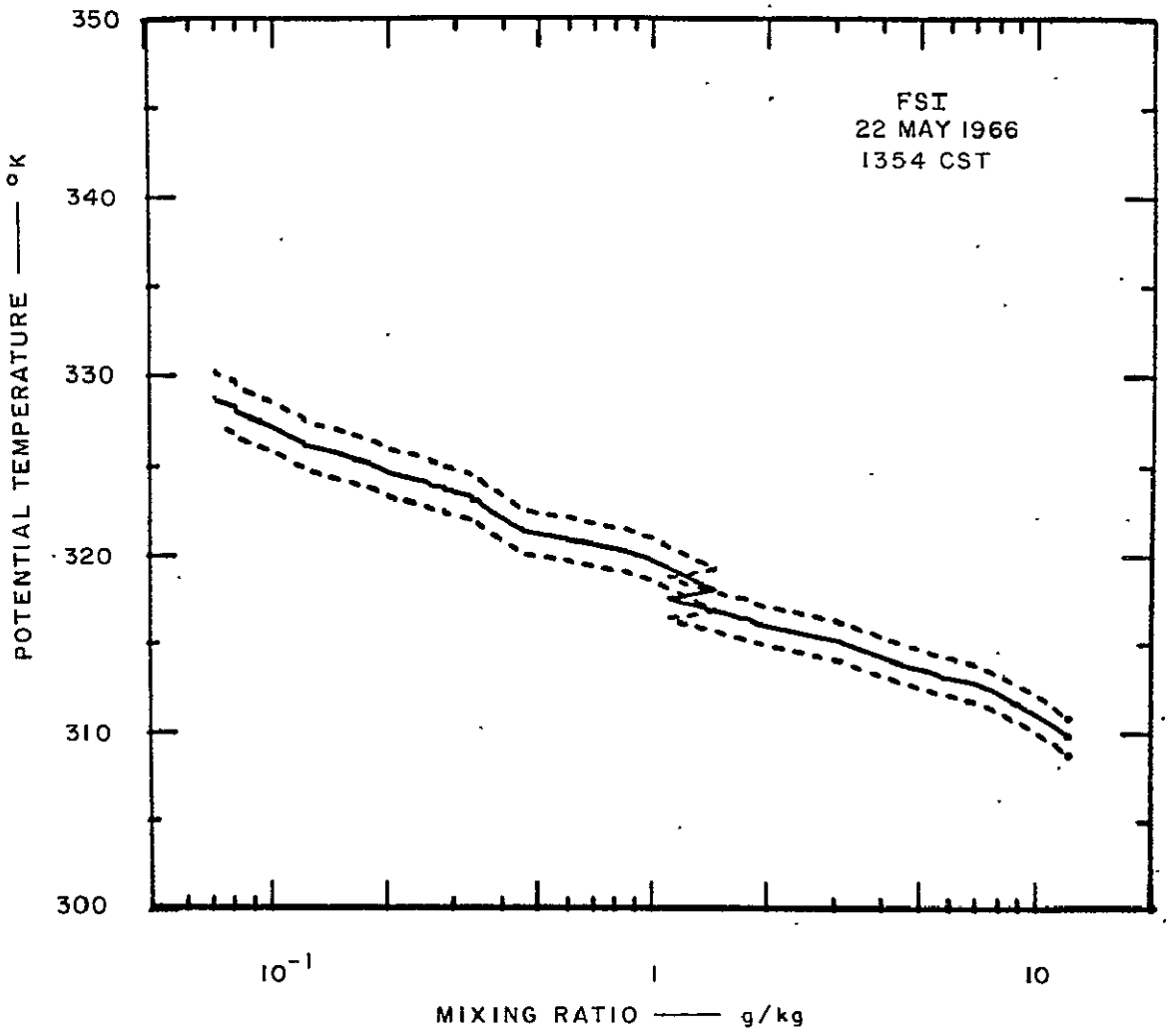

FIGURE 3 MIXING-RATIO PROFILE AS A FUNCTION OF POTENTIAL TEMPERATURE

Solid line shows the measured values while dashed lines show what the mixing-ratio profile would be if temperatures were in error by ±1°C.

D. Data Processing

Both the basic NSSL and AVE-II data had to be processed to place them in a form suitable for isentropic analysis and for tracking the mixing-ratio fields of the isentropic layers. This processing consisted of:

- Constructing isentropic profiles of the data
- Eliminating superadiabatic lapse rates
- Computing layer average data.

The elimination of superadiabatic lapse rates was performed whenever a θ point was found that was lower than the value just below it. The procedure used was to restructure a section of the θ profile between a top point that has a θ value greater than any values below it and a bottom point that has a θ value lower than any values above it. The restructuring was performed in such a manner that θ did not decrease with height, but yet the profile still retained the same average value for θ; that is, the area under the θ-p curve remained the same as illustrated in Figure 4. Over the layer that was mixed, average values for all other quantities, such as u, v, and m, were used throughout the layer. This frequently produced sharp discontinuities at the boundaries of the mixed layer and is probably not too realistic. However, tests showed that this mixing of u, v, and m had negligible effects on the final results of the study.

The layer thickness used for the NSSL data was $2\text{-}1/2^{\circ}$ and that for the AVE-II data was 4°. These choices were made largely for computational convenience, but also to keep the thickness of the layer significantly smaller than synoptic processes. An example of the θ layer profile along with the original θ profile is shown in Figure 5 for the station at Wichita Falls (a 5° layer thickness was used in this particular example). The layer average values from all the observing stations for a given isentropic layer were used to provide the basis for tracking the movement of a mixing-ratio field. The tracking technique that was used is described next.

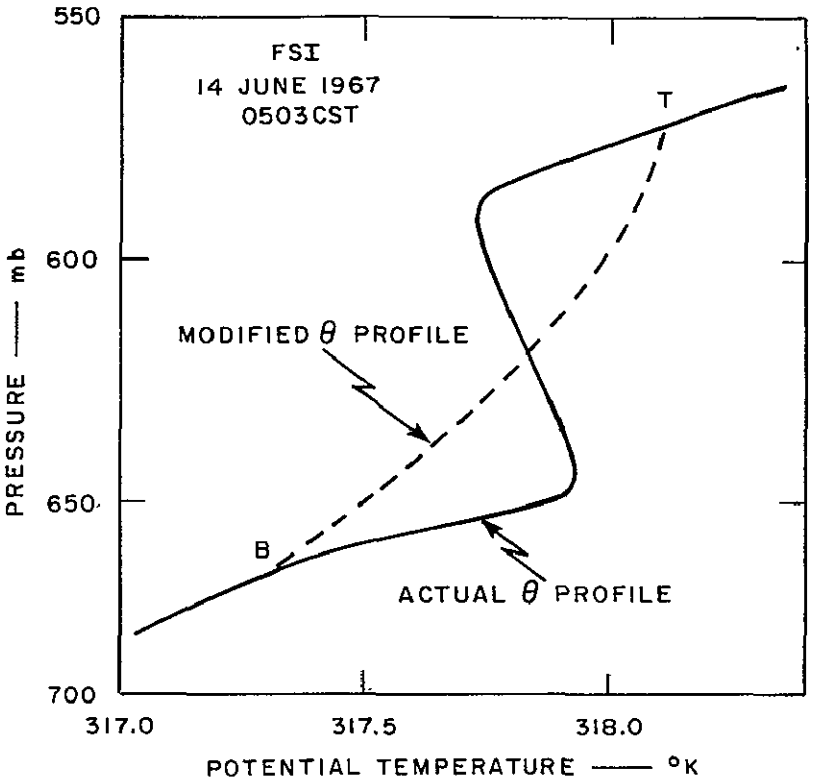

FIGURE 4 ILLUSTRATION OF TECHNIQUE USED TO MODIFY SUPERADIABATIC LAPSE RATES

The modified θ profile (dashed line) is a second-degree polynomial that fits the points B and T and that has an average θ value equal to that of the actual profile (solid line).

E. Tracking Technique

Automated tracking methods have been based either on clustering or cross-correlation concepts (Endlich et al., 1971; Leese et al., 1971). Both of these methods have been used at SRI, but the clustering technique has been preferred because it is more adaptable for use in tracking multilayer cloud motions. For this part of the study neither of these techniques was found to be suitable due to the small area that is covered

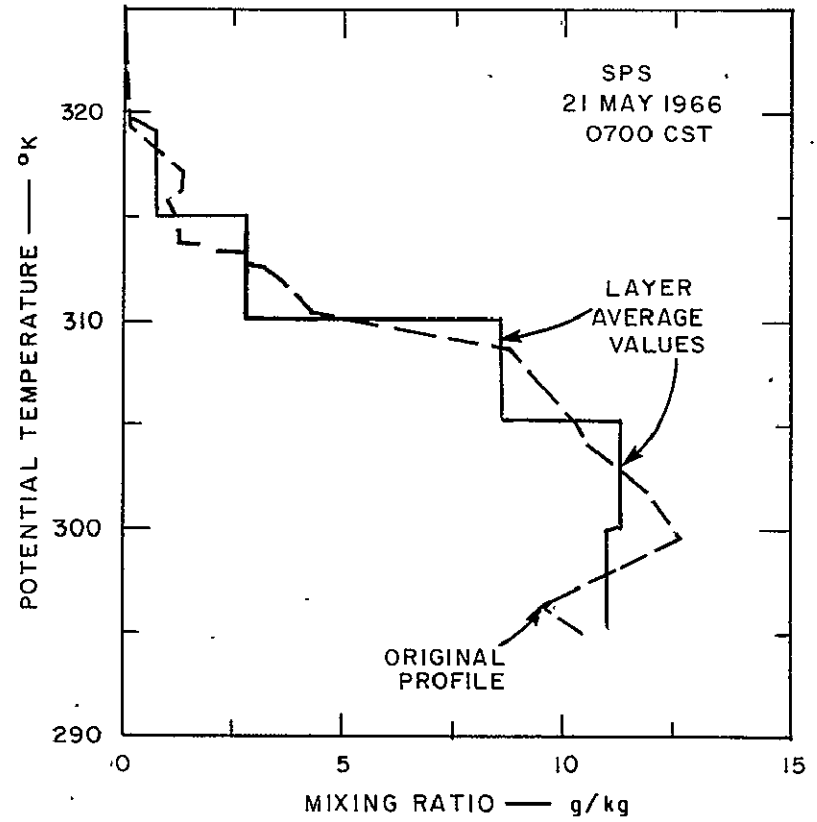

FIGURE 5 ILLUSTRATION OF LAYER AVERAGE AND ORIGINAL MIXING-RATIO PROFILES

by the NSSL-rawinsonde stations of Figure 1.* Visual tracking could have been used in this study; however, even this was found difficult, because many features observed at one time could move out of the region by the next time or change their appearance significantly. Also, visual tracking is subject to human bias.

Consequently, an objective least-squares fitting technique was developed for use with the type of data of this study. It consists of

---

*The ISODATA clustering or cross-correlation techniques, however, should be suitable for use with actual satellite data that would cover much larger areas. Section III proceeds on the basis that ISODATA will eventually be used in an operational system.

fitting to all the mixing-ratio (m) values that were available for one layer, a second- or third-degree polynomial surface that is assumed to move with the average wind components ($\bar{u}$, $\bar{v}$). The second-degree or quadradic polynomial surface is given by

$$m = a + bx_o + cy_o + dx_o y_o + ex_o^2 + fy_o^2$$

$$x_o \equiv x - \hat{u}t$$

$$y_o \equiv y - \hat{v}t \quad .$$

Thus, x_o and y_o are the initial x and y values at time t = o, and a, b, c, d, e, f, $\hat{u}$, and $\hat{v}$ are the unknown coefficients; $\hat{u}$ and $\hat{v}$ along with the other coefficients are determined so that the equation fits the data with a minimum mean-square error. Thus, the polynomial surface has a shape and moves at a velocity ($\hat{u}$, $\hat{v}$) that give a best fit to all the data. If the polynomial surface for the mixing ratio does actually move with the wind, then the coefficients $\hat{u}$ and $\hat{v}$ will be equal to $\bar{u}$ and $\bar{v}$. The method of Marquardt (1963) for least-squares fitting of nonlinear equations to a given data set was used to determine the coefficients. This method is an iterative one in which the coefficients are given a first-guess value. Its use permitted various higher-order polynomial forms to be conveniently tested. In tests that were carried out, higher-order polynomials in either t or x and y were found to give better fits to the data, but they were also found to be more unstable and to give poorer estimates of the wind. The above quadratic equation generally gave better results because of its tendency to provide a very strong smoothing of the data. In the application of this technique it was found to be important for:

- The interval between observations to be sufficiently small so features at one time will not be advected completely outside the area by the next time. This permits continuity

to be maintained between times and an effective orverlapping of data, which is important because of the changing nature and the errors of the data.

- The total time span of the data not to be too long in order that a second-degree polynomial field moving through the region can give a reasonably unique fitting of the data.
- The first-guess values for $\hat{u}$ and $\hat{v}$ to be as reasonable as possible. The iterative technique can give different solutions depending on the first-guess values and may occasionally give inferior results if a zero or a poor first-guess value is used.

The above method was found to give satisfactory results, particularly if the data were consistent in space and time. An example is shown in Figure 6 for the 317.5-320.0° isentropic layer of 22 May 1966. In the first column of the figure (a) computer isopleth analyses of the actual mixing-ratio values are shown. During this period, the NSSL soundings were taken at 1-1/2 hour intervals over a total period of six hours. (Soundings were not taken at the second time, 1230 GMT, and an interpolated field is shown for this time in the first column.) The average wind speed and direction were 16.2 m s^{-1} and 265°. In the second column of the figure (b) isopleths are shown for the second-degree polynomial surface that gave the best fit to the data. This surface moves with a speed and direction of 18.5 m s^{-1} and 263° in close agreement with the actual wind. Also, it gives a reasonable representation of the actual fields in the first column, although considerably smoothed. In the third column of the figure (c) isopleths are shown for a third-degree polynomial surface. This gives a better fit to the actual data, but does not move in as good agreement with the wind.

F. Case Studies

The NSSL and AVE-II special soundings programs have provided unusually good sources of data; however, they were carried out during severe-storm weather conditions. NSSL cases appropriate for this study occurred

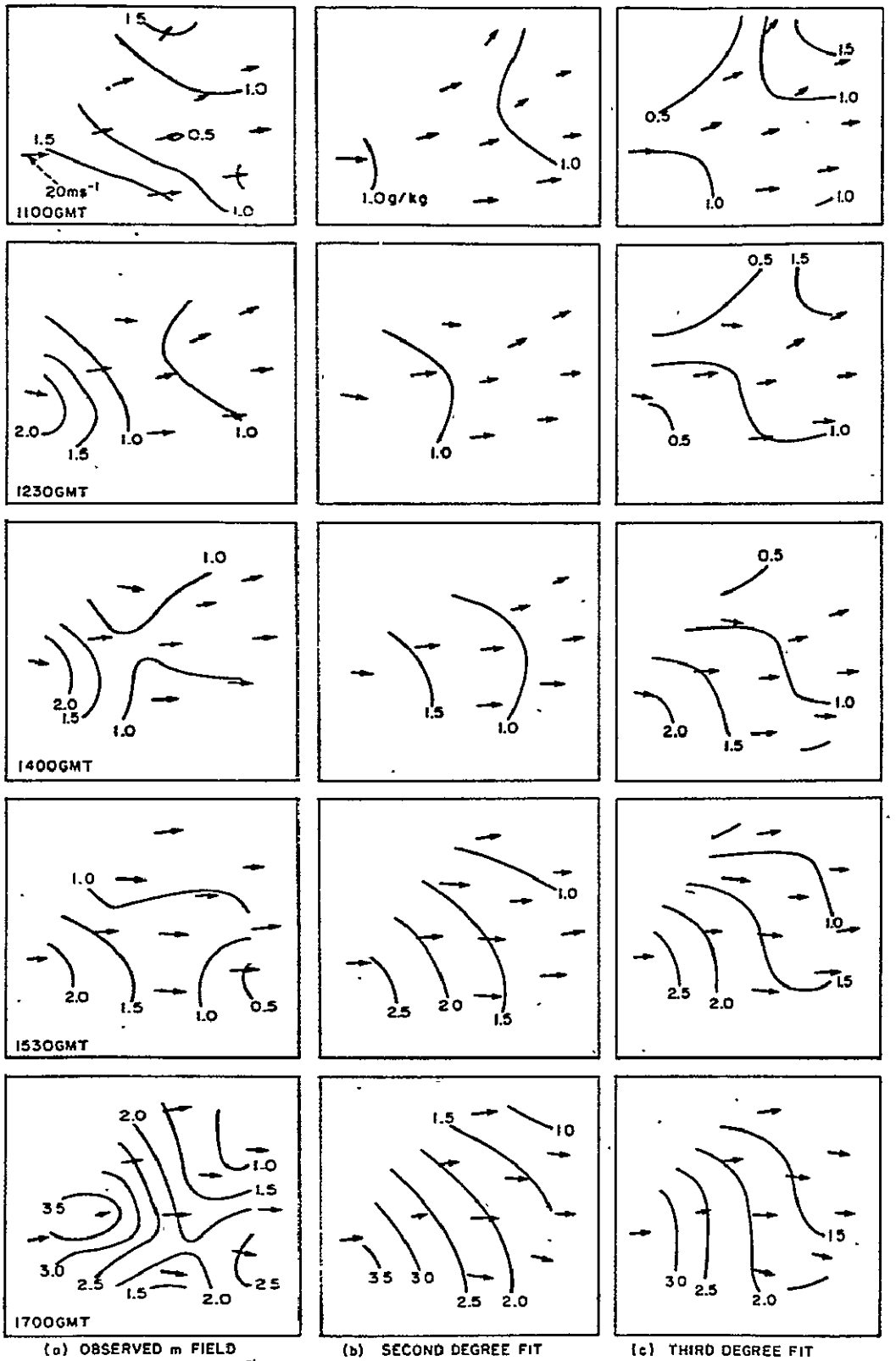

FIGURE 6 COMPARISON OF OBSERVED MIXING-RATIO FIELDS (COLUMN (a)) WITH A SECOND- AND THIRD-DEGREE POLYNOMIAL FIT (COLUMNS (b) AND (c)) FOR THE 317.5-320.0° ISENTROPIC LAYER, 22 MAY 1966

The polynomial surfaces for the mixing-ratio move with a speed and direction that gives the best fit to the data. The mixing-ratio isopleths are labeled in g/kg and the vectors denote the actual winds at each station (vectors are identical in each column).

only when the forecast was bad and when extensive soundings were made in relatively good weather. This did not occur often and restricted the data that could be used to only a few NSSL cases in addition to a small section of the AVE-II area. Cases were selected on the basis of relatively cloud-free conditions. This, however, was difficult to determine accurately, even when using available satellite imagery.

1. NSSL Case, 22 May 1966

The NSSL weather summary as given by Barnes et al. (1971) for this period was as follows:

> Early morning radar echoes dissipated by 0900 CST. Southerly flow continued strong during the day with a low-pressure trough forming in western Oklahoma. The flow at 500 mb was mainly westerly. Serial soundings were started at 1100 and terminated after 1700. There was no radar activity over the network on this day.

A nephanalysis for 1254 CST, 22 May 1966, that was derived from the ESSA-1 satellite photographs indicated some low and high clouds, but generally open skies over most of the network's area. Figure 7 shows the vertical profiles of potential temperature . mixing ratio, and relative humidity for FSI; only the profiles for the beginning and ending of the period (1110 and 1700 CST) are shown. Initially, there were two vertical layers containing similar moisture characteristics; one from the surface up to an inversion at about 850 mb and another from about 850 to 550 mb. By the end of the period, the lower inversion had broken, and considerable vertical mixing occurred with an overall increase in moisture. It would appear that an increase in cloudiness also occurred near the end of the period. This 22 May period provided a reasonably good case, with 10 stations reporting.

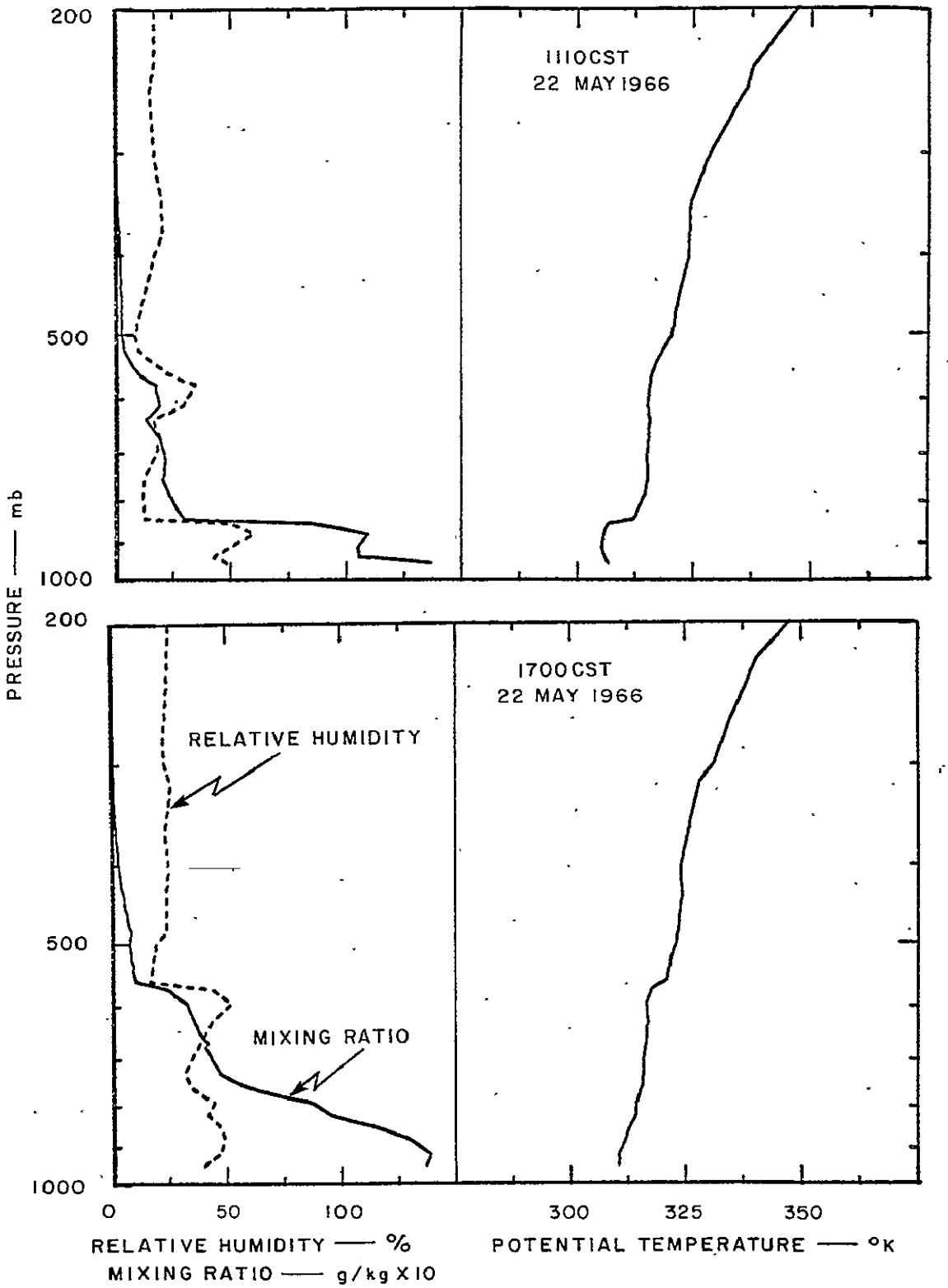

FIGURE 7 VERTICAL PROFILES OF POTENTIAL TEMPERATURE, MIXING RATIO, AND RELATIVE HUMIDITY AT FORT SILL, OKLAHOMA, 22 MAY 1966

Profiles of isentropic humidity motions were computed for this 22 May 1966 period, using the tracking technique described previously in Section E. The results for the humidity tracking are shown in Figure 8.

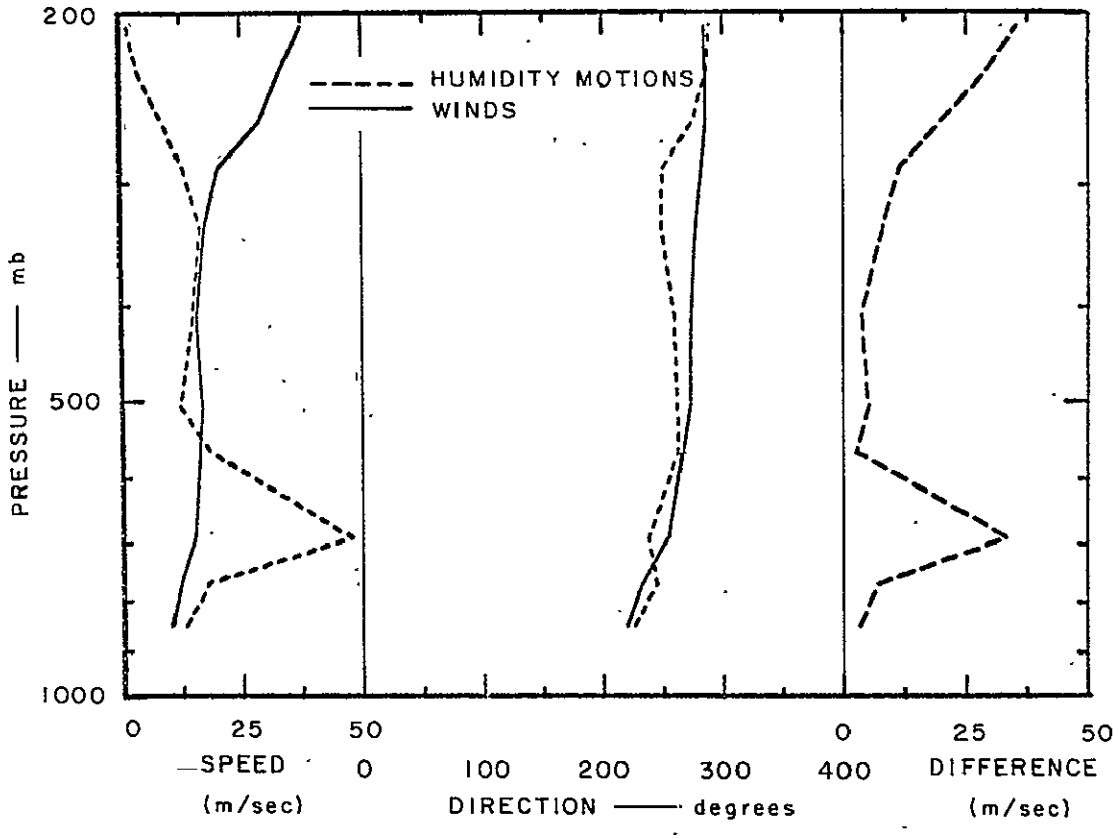

FIGURE 8 COMPARISON OF HUMIDITY MOTIONS IN ISENTROPIC LAYERS WITH ACTUAL WINDS, BASED ON NSSL DATA FOR 1100 TO 1700 CST, 22 MAY 1966

The profiles for the actual average wind direction and speed (solid lines) are shown along with those estimated by tracking the mixing-ratio field (short dashed lines). Also shown are the magnitudes of the vector differences between the two (long dashed lines). The profiles are shown as a function of pressure rather than potential temperature. This was done by using the average pressure for a θ layer. The two profiles for direction in Figure 8 show excellent agreement; the difference being less

than 30° at all altitudes. However, the humidity motions overestimated the wind speed in the lower troposphere below about 600 mb where unstable conditions had existed, and the isentropic concept was probably invalid. Above this level the humidity motions provided a good estimate of the wind speed (to within 20 percent) until about 300 mb. At this level, they started to give an underestimate of the actual wind speeds. This effect shows up in all of the cases studied. If the patterns were being tracked on a constant height or pressure surface (rather than a θ surface), one would expect a tendency for the results to give an underestimation of the wind speeds above about 500 mb. This is because the air usually moves faster than the weather systems in the upper troposphere. However, the tracking speed estimates above 300 mb in Figure 8 are too low to be consistent even with the movements of weather systems. It appears rather that this effect is associated with the fact that the humidity measurements become increasingly more unreliable at higher altitudes, and it is probably produced by systematic errors associated with each station, since the results tend to show features that persist in time.

An experiment was also carried out in which the tracking was performed using the mixing-ratio values for constant pressure layers rather than isentropic layers. The results for this experiment are shown in Figure 9. The comparison, particularly with wind speed, is not as good as that in Figure 8, implying that it is important to perform the tracking of mixing ratios using an isentropic layer or surface. In another experiment, an attempt was made to track $\partial p/\partial\theta$ values of isentropic layers ($\partial p/\partial\theta$ is conserved in a nondivergent flow). The results showed little agreement between the profile for the $\partial p/\partial\theta$ motions and the real wind; although the discrepancy was least in the 600 to 400 mb region. This suggests that divergence is a significant quantity that cannot be neglected.

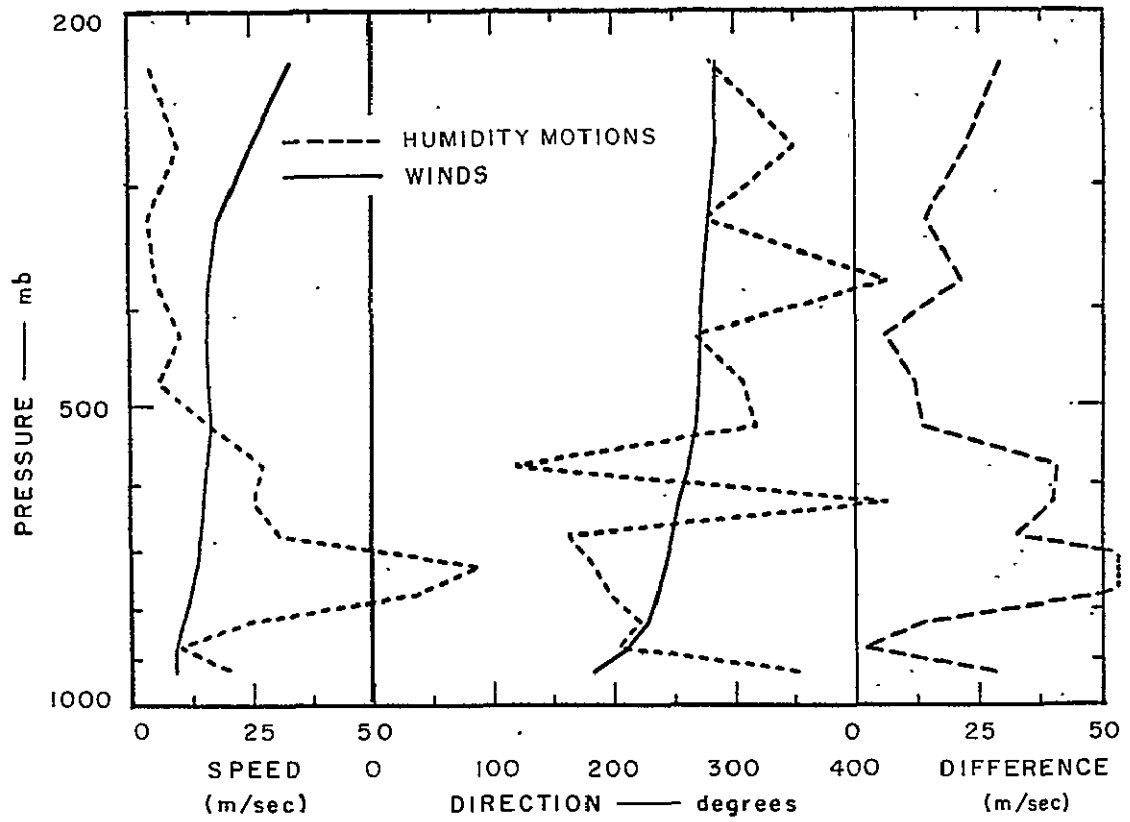

FIGURE 9 COMPARISON OF HUMIDITY MOTIONS IN CONSTANT PRESSURE LAYERS WITH ACTUAL WINDS, BASED ON NSSL DATA FOR 1100 TO 1700 CST, 22 MAY 1966

2. NSSL Case, 14 June 1967

The NSSL weather summary for this period was as follows:

> Serial soundings were begun at 0500 in the morning and soundings were taken every three hours until after 1700. Moderate southerly flow continued over the state as a cP front approached from the northwest. At 500 mb, the flow backed into the south as a short wave approached from the west. There was no radar activity.

The ESSA 5 satellite photograph for 1523 CST, 14 June 1967, showed generally scattered clouds, however, a large cloud mass appeared to extend into the northwest of the area. Figure 10 shows the vertical profile of potential temperature, mixing ratio, and relative humidity for FSI at

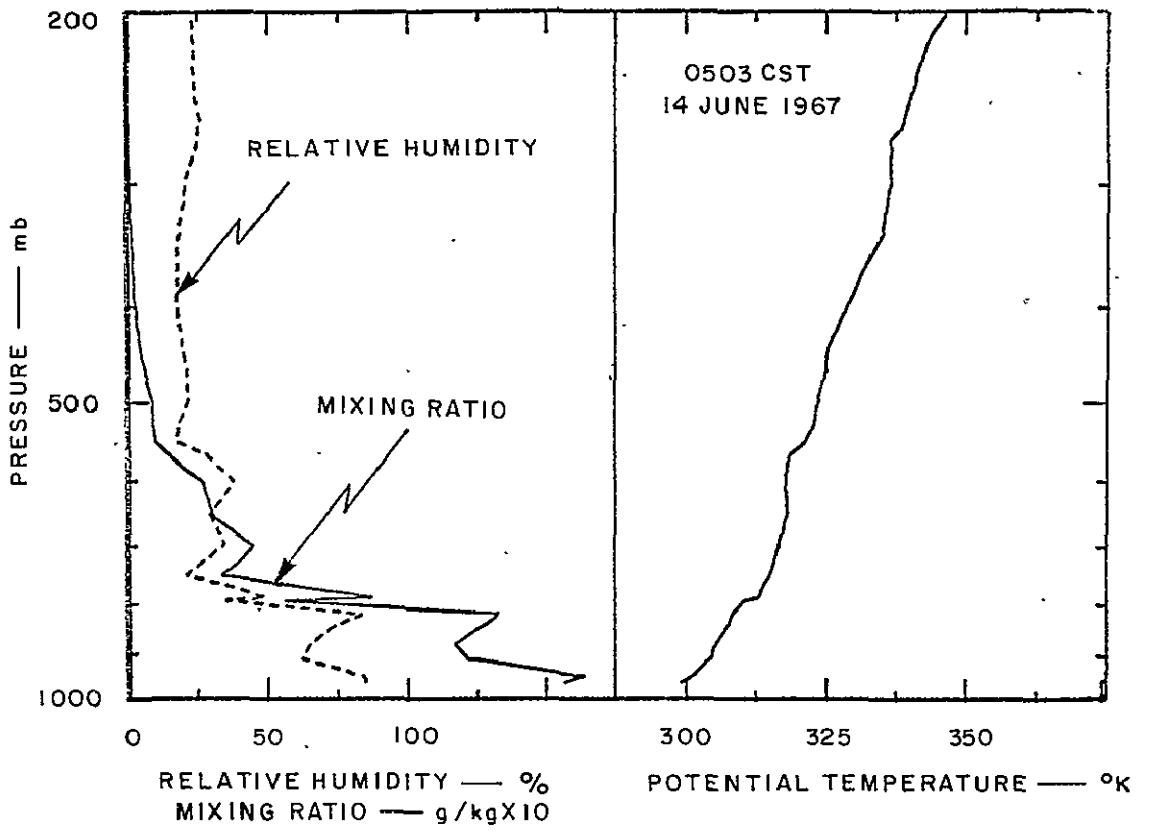

FIGURE 10 VERTICAL PROFILES OF POTENTIAL TEMPERATURE, MIXING RATIO, AND RELATIVE HUMIDITY AT FORT SILL, OKLAHOMA, 14 JUNE 1967

0503 CST, 14 June 1967. These profiles show a relatively moist layer below about 800 mb, that is slowly becoming superadiabatic. Near-adiabatic layers also exist at about 600 and 300 mb that break down in later soundings.

The results for the humidity tracking experiment are shown in Figure 11a. The estimated wind directions were rather erratic, giving

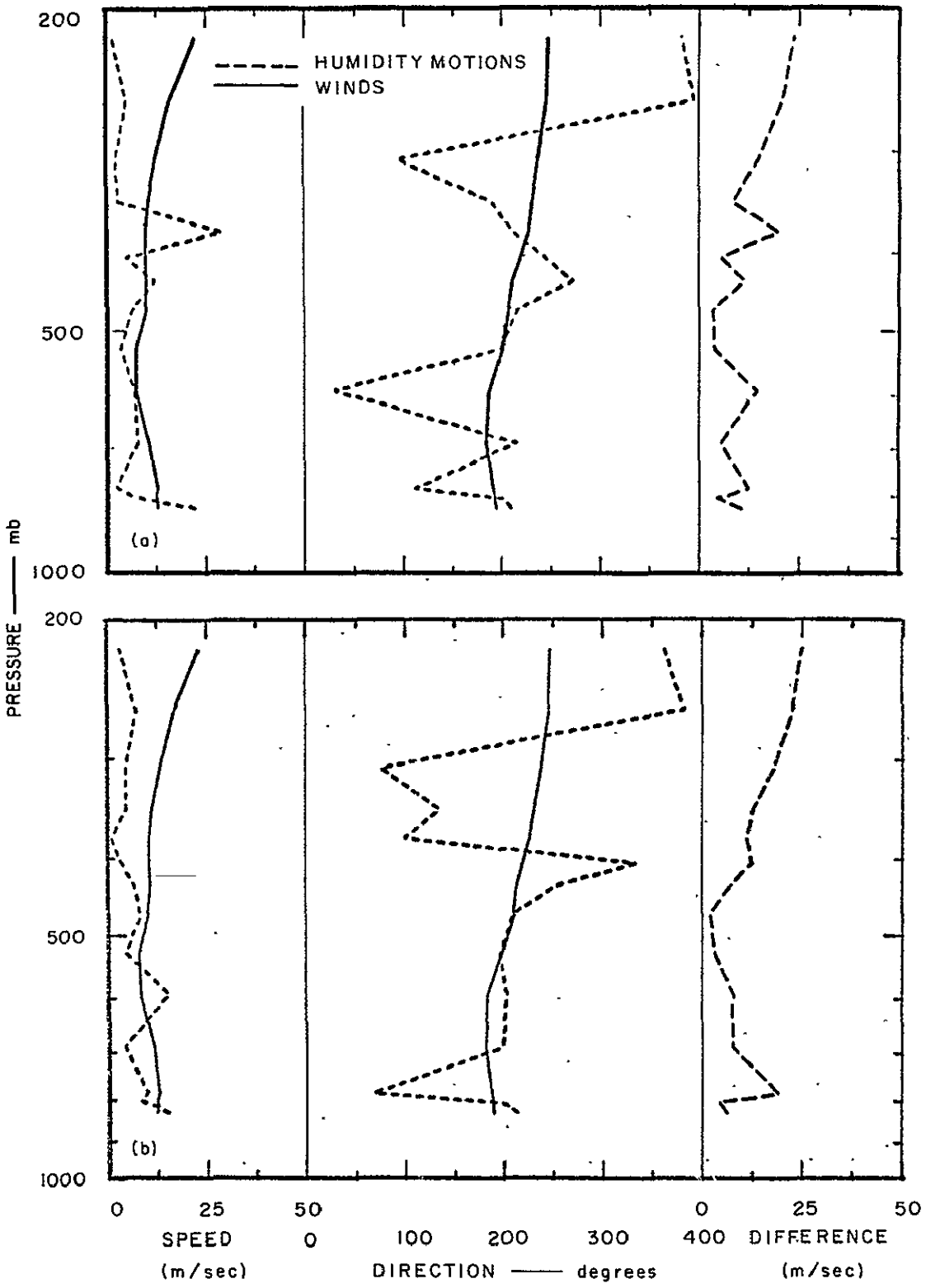

FIGURE 11 COMPARISON OF ISENTROPIC HUMIDITY MOTIONS WITH ACTUAL WINDS, (a) BASED ON NSSL DATA FOR 0500 to 1700 CST, 14 JUNE 1967, AND (b) BASED ON NSSL DATA FOR 0800 to 1700 CST, 14 JUNE 1967

poor results near the surface, and at 600 and 300 mb where near- or superadiabatic conditions had existed at the beginning of the period. A high peak in the humidity motions occurs at about 350 mb, but again they underestimate the wind speeds in the upper troposphere above this level. An improvement in the results occurs, particularly at 600 mb, if the data for the first observation time are omitted, as shown in Figure 11b. However, these results are not as good as those for the previous NSSL case. This appears to be attributable to the instability of the atmosphere during this period and to the cloudiness. Also, the interval between soundings for this case (three hours) was long relative to the network size, resulting in little time continuity and a relatively long total period of 12 hours.

3. Other NSSL Cases

The NSSL period for 25 April 1967 was also investigated. This case had thunderstorms and strong radar echoes just outside the network. Only six stations were reporting, and strong winds even at low altitudes carried the patterns completely out of the area during the interval between observations (1-1/2 hours). Also, some of the soundings apparently entered convective clouds and gave highly unrepresentative values. Thus, this case of 25 April was not too suitable for the study, but an attempt was made to eliminate the humidity measurements that were inconsistent with surrounding data and to track the mixing-ratio field. The computation of humidity motions still gave erratic results and little agreement with the actual wind. All other cases as described by NSSL for 1966 and 1967 either had storm activity or too few soundings; thus, they were not tested.

4. AVE-II Case, 12 May 1974

The AVE-II experiment was also carried out during severe weather conditions, but a section of the area had relatively clear skies during

the latter half of the period (0000 to 1200 GMT, 12 May 1974). The surface synoptic charts for 0000 and 1200 GMT, 12 May 1974, are shown in Figure 12. The NOAA-3 satellite visible imagery for 0900 local times (1500 GMT for the CST zone) on 12 May 1974 is shown in Figure 13. A relatively clear region is behind the cold front in the western part of the AVE-II area (the IR imagery indicates that only low cloudiness existed there). The stations that were used in this study were previously shown in Figure 2. These stations were selected because they were believed to have reasonably clear skies and to give an isentropic surface with a range of altitudes that would not be too great. The group of stations directly south of these might also have provided a good selection since Figure 13 indicates clear skies. However, these stations covered a region containing different air masses, particularly noticeable in the 850 and 700 mb synoptic maps.

The vertical profiles of potential temperature, mixing ratio, and relative humidity for Omaha (OMA) at the beginning and ending of the period are shown in Figure 14. The lower troposphere was relatively moist and not very stable at the initial time. However, as the front moved further away, the atmosphere cleared and stabilized. The results for the humidity tracking experiment are shown in Figure 15. The directions for the winds and the humidity motions are in excellent agreement. The speeds show very close agreement between 700 and 500 mb. However, in the unstable and moist region below 700 mb, the humidity fields moved faster than the wind. Above 500 mb, the humidity speeds as in previous cases became increasingly too low. These results are similar to those for the NSSL case of 22 May 1966.

An experiment was also carried out using this case to test the effect of tracking relative humidity rather than mixing ratio. Although relative humidity is not strictly a conserved quantity, it does have the advantage of having similar magnitudes throughout the troposphere; that

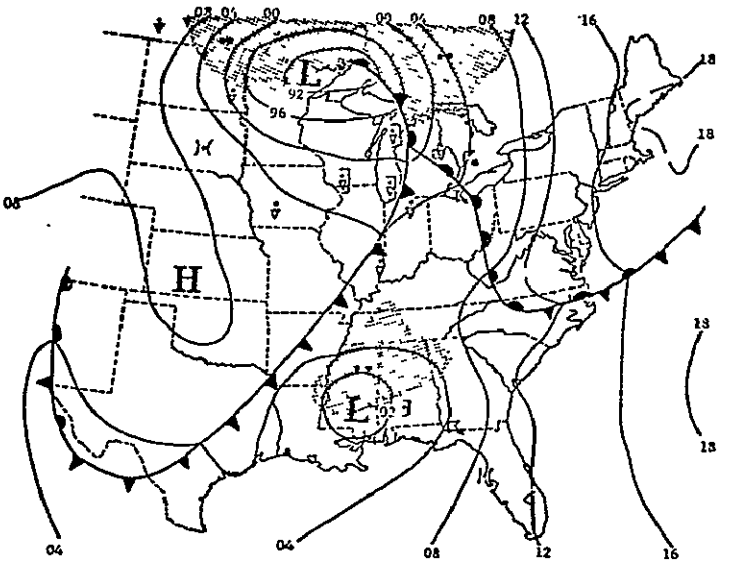

0000 GMT

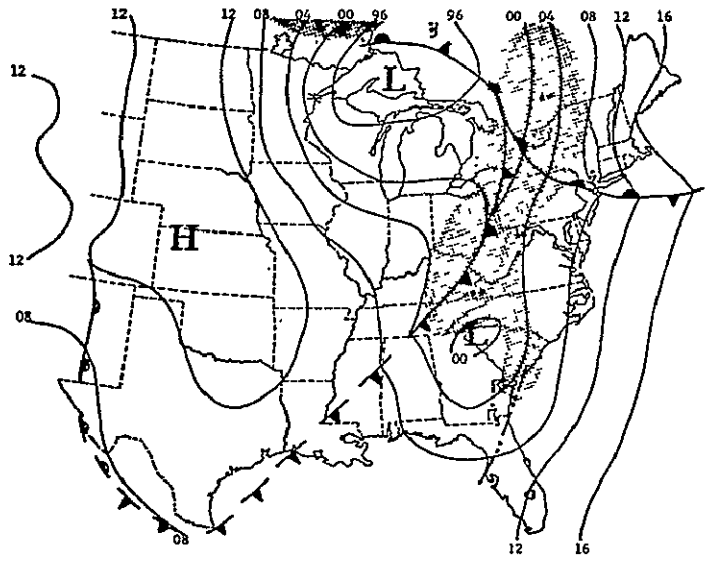

1200 GMT

FIGURE 12 SURFACE SYNOPTIC CHARTS FOR 12 MAY 1974

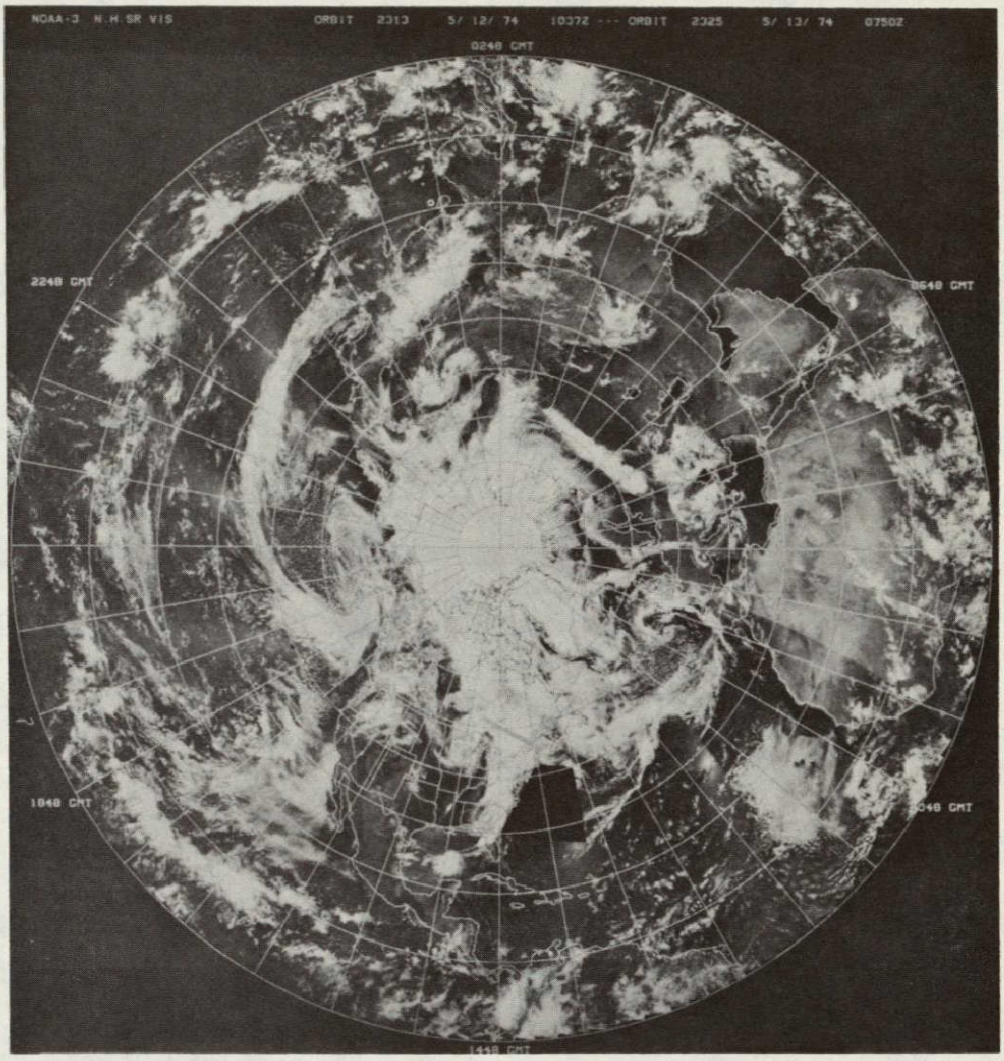

SA-3529-15

FIGURE 13 NOAA-3 NORTHERN HEMISPHERE MOSAIC FOR 0900 LOCAL TIMES (~1500 GMT OVER CENTRAL U.S.), 12 MAY 1974

is, unlike mixing ratio it does not decrease rapidly with height. Thus, if it were at least quasi-conserved it might serve as a more practical tracer of circulation than mixing ratio. The results of this experiment are shown in Figure 16. They are similar to those obtained for

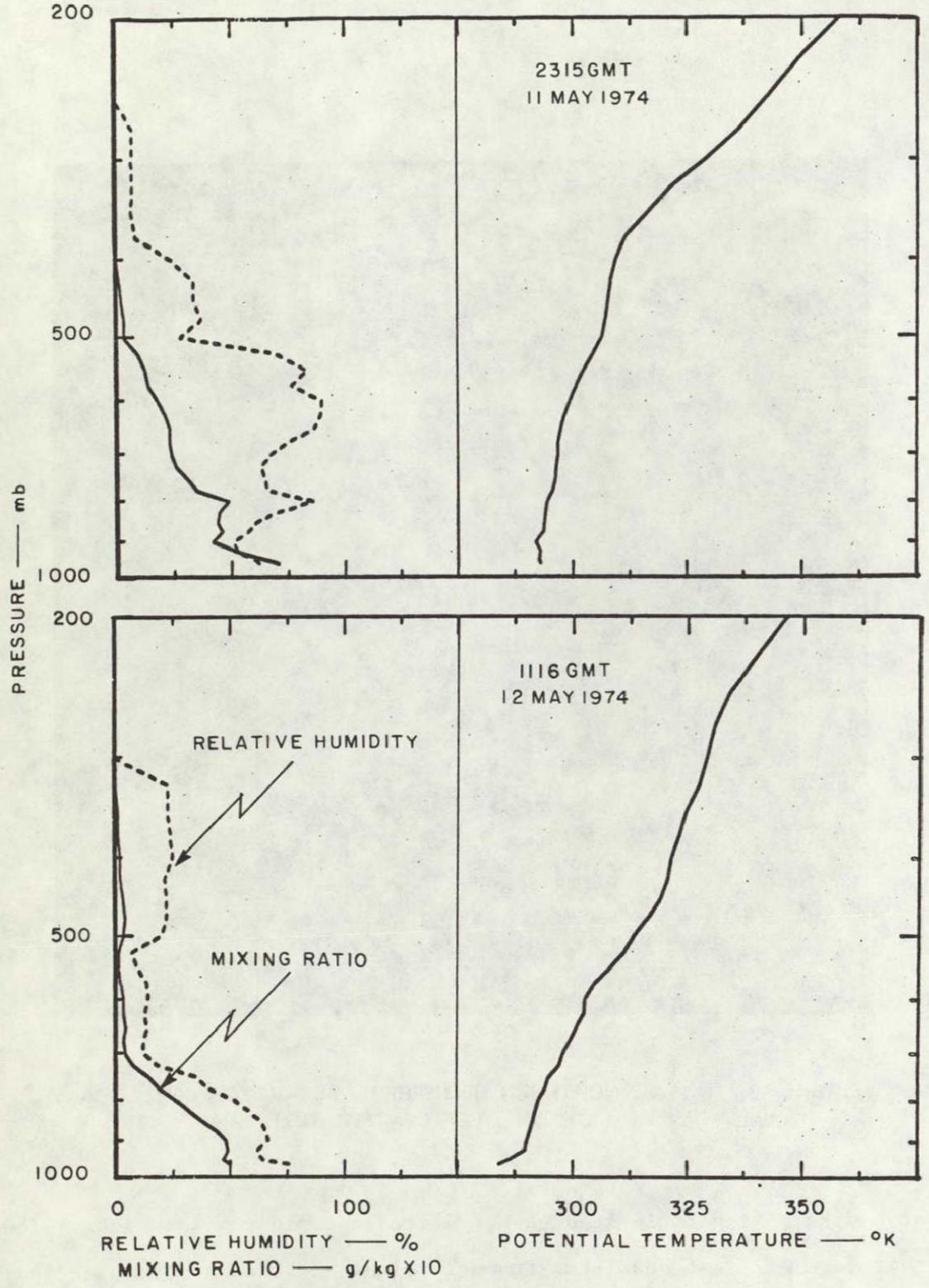

FIGURE 14 VERTICAL PROFILES OF POTENTIAL TEMPERATURE, MIXING RATIO, AND RELATIVE HUMIDITY AT OMAHA, NEBRASKA, 12 MAY 1974

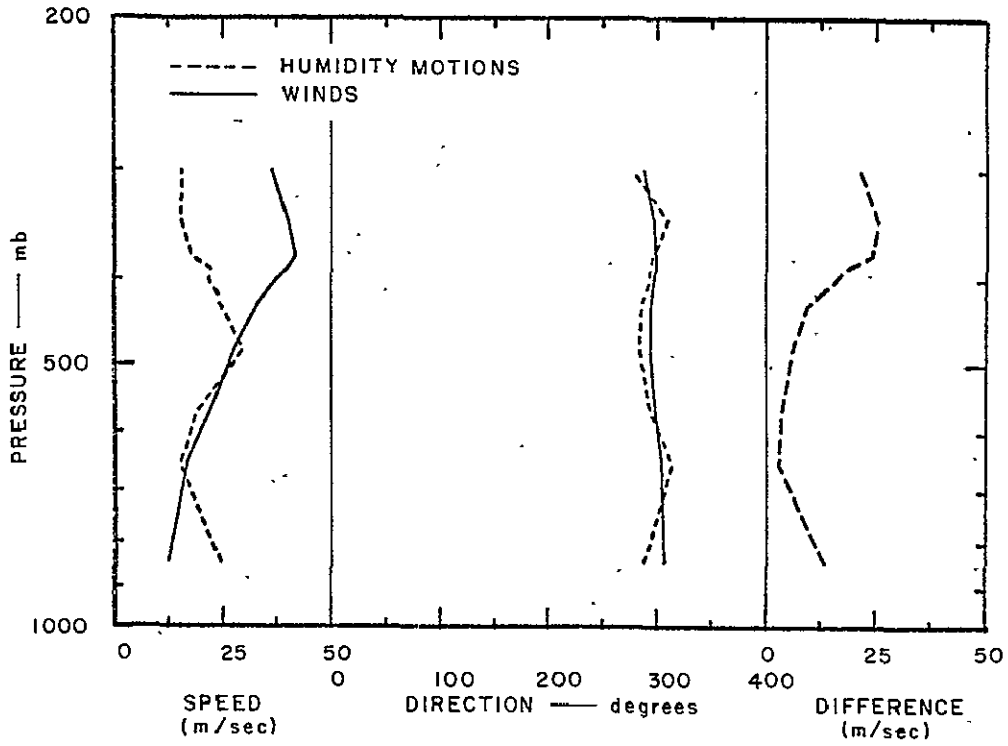

FIGURE 15 COMPARISON OF ISENTROPIC HUMIDITY (MIXING RATIO) MOTIONS WITH ACTUAL WINDS, BASED ON AVE-II DATA FOR 0000-1200 GMT, 12 MAY 1974

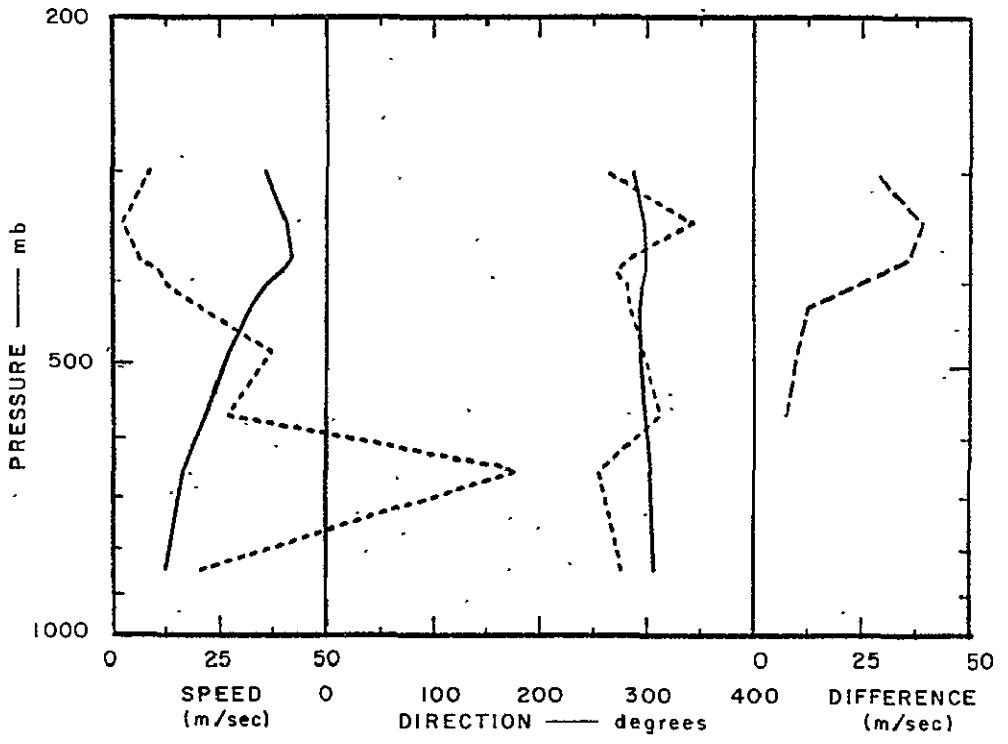

FIGURE 16 COMPARISON OF ISENTROPIC HUMIDITY (RELATIVE) MOTIONS WITH ACTUAL WINDS, BASED ON AVE-II DATA FOR 0000-1200 GMT, 12 MAY 1974

tracking the mixing ratios of a constant pressure layer (Figure 9). That is, the humidity directions look reasonable, but the humidity speeds considerably overestimate the actual winds in the lower troposphere and underestimate them in the upper troposphere.

5. Low Vertical Resolution Profile Data

In the previous experiments, results were obtained for small θ intervals, assuming that the vertical resolution of a satellite sounding could be relatively high. However, a satellite sounding would probably have a vertical resolution of seven layers at most. Even in the near future, satellite systems with a degraded resolution of three layers or less may be used. To examine the effects of such a system, an experiment was carried out using the AVE-II data. (The AVE-II data set was chosen since it had data spacings more comparable to what might be expected with a low-resolution satellite system.) The soundings were divided into three θ layers: approximately from the surface to 700 mb, 700 to 500 mb, and 500 to 300 mb. However, tracking of humidity patterns could not be performed for the lower and higher isentropic layers. In the lower layer this was because of the steep slope of the layer and its interception with the earth's surface, while in the upper layer the humidity measurements are unreliable. Thus, meaningful tracking could only be carried out with the middle θ layer (306° to 318°). The result was that the computed humidity motion was in agreement with the wind of the lower part of the layer; the average mixing-ratio value of the layer is determined mainly by the mixing-ratio values in the lower levels, which have much higher values. Thus, tracking of mixing ratios for a thick layer is nearly equivalent to tracking them for a thin layer at the bottom. Degraded resolution both in the vertical and horizontal would restrict the application of the humidity motion concept, although at least one motion measurement at approximately 600 or 500 mb should be possible

in cloud-free areas. This is important, however, since this is the level at which wind information is most needed, particularly in the tropics, to supplement cloud motions, which are generally available for the 850 and 200 mb levels (Thompson, 1971).

G. Summary and Recommendations

The principal results of this study indicate that humidity motions are in close agreement with winds under the proper conditions, particularly near the 500-mb level. These conditions are when there were few clouds, minor non-adiabatic influences, and enough moisture to be measurable. In the lower troposphere, the humidity motions were unreliable due to non-adiabatic effects and the frequent existence of adiabatic or superadiabatic lapse rates. In the upper troposphere, the humidity measurements were associated with cold temperatures and the water vapor amounts were too low to be measured with enough reliability for tracking.

Thus, wind determination by tracking isentropic humidity patterns appears to be feasible in the mid-troposphere, and to have application over large regions of the globe, especially the tropics. Selection of favorable locations, that is where there are few middle clouds and stable lapse rates, could be made using satellite cloud photographs and humidity temperature profile measurements. If the satellite profile measurements provide better coverage in space and time than rawinsonde data, the feasibility and the accuracy of the tracking will be increased. Also, the humidity motions could be used in computing balanced heights in the mid-troposphere, and these heights could in turn be applied as a reference level for the temperature height profiles (Endlich et al., 1972c).

Further comparisons of humidity motions with winds are needed in order to confirm the results of this study, and to determine more exactly the conditions under which the humidity motions can be used with confidence. Special upper-air rawinsonde observations were made by the U.S

Army during October and November 1974, using a meso-network that was established at White Sands, New Mexico. These data should provide a good source for carrying out further investigations, since the upper-air observations were frequently made during stable and clear-sky conditions. However, verification and experience with actual data from a geosynchronous sounder will still be required.

The technique used to track the mixing-ratio field in this part of the study consisted of finding a second-degree polynomial representation of the field that moved with a speed and direction to give a best fit of the data. The method worked well and was ideally suited for use with the type of data that was available. It could possibly be used for tracking actual satellite measured mixing-ratio fields in real time. However, it would be necessary to develop a more efficient and modified scheme and to compare it with other techniques for both efficiency and accuracy.

A similar approach to that given above for determining tropospheric motions can be made for the stratosphere using satellite measurements of ozone. Ozone below 25 km is a quasi-conservative property of the air and has been known for some time to have an application as a natural tracer of atmospheric motions (Hering, 1965). Thus, by tracking ozone on isentropic surfaces, it should be possible to derive stratospheric winds for use in numerical prediction models. Total ozone measurements have been made successfully with the Nimbus 3 and 4 satellites (Conrath et al., 1970; Heath et al., 1974). In particular, the ozone data derived from the backscatter ultraviolet (BUV) experiment of the Nimbus 4 provides spatial distributions of atmospheric ozone, including vertical structure, on a global basis. Such data, when combined with the available temperature profile data, should permit investigations of the large-scale transport of ozone.

III AUTOMATED TRACKING OF HUMIDITY FIELDS USING PATTERN RECOGNITION TECHNIQUES

A. Review of Tracking Techniques

Tracking can be performed with reasonable accuracy by a keen human observer using interactive time-lapse imagery analysis equipment (Evans and Serebreny, 1969; Evans, 1975). However, because of the vast quantities of data, automated methods of tracking must be developed that will be able to replace many or all of the human tracking decisions. The dynamic clustering method, ISODATA, developed at SRI shows promise in this regard (Endlich et al., 1971; Wolf et al., 1973). Other automated tracking techniques are based on the cross-correlation method (Leese et al., 1971), including the Fourier transform method that is used as a means of rapidly computing cross-correlations (Arking et al., 1975). The University of Wisconsin has developed a man-machine system (Smith and Phillips, 1972) for tracking, and this also is based on a correlation approach.

B. Nature of Humidity Fields

1. Definition of Humidity Packets

As a convenience, one can always define thresholds of humidity around regions of higher or lower humidity. Fields of humidity above (or below) threshold are probably similar in appearance to cloud fields. Thus, the tracking of humidity fields and clouds can be regarded as fundamentally the same. To distinguish these regions of high (or low) humidity from clouds, they are referred to as packets of humidity in this report. The existence of such packets and their similarity to clouds is supported by the THIR 6.7 μm imagery (Steranka et al., 1973).

2. Significance of Data Density

A high density of data implies long and costly computer processing times. However, it is more likely that there will be too little of the retrieved temperature and humidity profile data, rather than too much. Satellite profile data are at present coarsely spaced at about 150 mile intervals. With sparce data, it is difficult to define humidity packets, and it may be conceptually better to think of gradients or trends. Future satellite measurements may be able to provide a higher density of profile data, at about 75 mile intervals. This is a significant increase, but it still does not approach the detail available in cloud imagery.

3. Tracking of Non-Rigid Bodies

The accuracy of a tracking system depends primarily on the entity or body being tracked. For example, if a rigid body is being tracked, the motion can be more accurately described than if the body is non-rigid or flexible, as is the case with clouds or humidity packets. It was demonstrated in a previous study by Hall et al. (1972) that the accuracies of tracking methods are high, and are limited only by the image resolution when applied to rigid-body tracking, as in landmark-matching applications. However, non-rigid bodies, such as humidity packets, can change in appearance from one time to the next due to non-adiabatic effects or to error. In such cases, the tracking will not be as accurate. Also, a mixture or complexity of motions in the field affects tracking ability, with multiple layers of motions being the most difficult. The preferable approach to tracking simple rigid bodies is by means of a cross-correlation technique using literal data of the highest resolution. However, the clustering approach appears to be preferable for tracking non-rigid bodies and complex motion fields, because statistical descriptors can be used that best represent the changing shapes and brightness of drifting packets.

C. ISODATA Program for Dynamic Clustering

1. General Description

The computer program known as ISODATA, performs a dynamic clustering analysis of data sets at successive time intervals for the purpose of tracking and computing motions. Clustering is a process of finding local averages or centers of relatively high concentration in a complex data set that contains many details. The local averages represent all the local data approximately, and thus clustering results in a compression of the data to its essentials. The process is called dynamic because it also links corresponding clusters at successive times and produces motion vectors. A more detailed description of ISODATA is given by Hall et al. (1973).

In matching clusters at successive times, a "fit factor" was devised, which is a measure of the similarity between two cloud clusters. It is based upon clustering statistics, such as number of points and average brightness. These are abstract quantities since they are aggregate counts and statistics rather than the literal data themselves. The fit factor and the choice of elementary statistics that go into it, and the way they are combined, are of chief importance. Ideally, one must choose a fit factor formulation that matches the stability of the data being tracked. If rapidly varying features are being tracked, then a literal approach would not result in sufficient recognition, so a more abstract set of statistics (perhaps even skewness and kurtosis) is more suitable for recognition, and allows a saving of computer processing time. There is some degree of variation of features beyond which tracking with fixed time intervals is not possible at all. Packets or clouds may completely disappear or appear, and tracking under these circumstances is meaningless, unless data is obtained more frequently. Since the time between data sets is usually fixed or beyond control, the specificity of the statistical descriptors used must be consistent with the life and rate of change of the features.

2. Accuracy and Efficiency

In dynamic clustering, the problem is to track a time-varying entity, such as humidity, with efficiency and accuracy. The current ISODATA program uses a threshold for the fit factor to compromise between accuracy and density of motion vectors. By varying this threshold, either a high or low density of vectors can be obtained. Since the vectors are ranked in order of their fit factor values, the choice of a lower density or smaller number of vectors would result in the most accurate ones. The threshold value for the fit factor is set by experience with the program.

Ideally, the number of clusters should be varied according to a clustering characteristic curve, to find the optimum number of clusters for each area and turbulence condition. This is an exhaustive approach, but it is guaranteed to find the optimum solution. However, optimum solutions can rarely be expected in practice, especially considering the computational costs and need for rapid results. Thus, the number of clusters that the program will delineate is, in practice, also an empirical choice that works best for typical cases.

Extensive comparisons of results from automated tracking with those from careful human visual tracking have not yet been made. Thus, it is not possible at present to make definite statements on the actual accuracy of the method. However, automated tracking accuracies should eventually be able to approach those that are obtained visually. Later in this section some experimental tracking results are given on the accuracy of the dynamic clustering method using simulated data.

With regard to the efficiency of ISODATA, it is estimated that the daily computer time used on a CDC 6400 would be about one hour for operating a tracking system that provides motions at three levels over a satellite-viewed earth disk. The daily cost using the SRI/CDC 6400

billing algorithm would be about $550. These figures do not consider the temperature and humidity retrieval computations.

D. Simulation of Humidity Data from Satellites

1. The Purpose and Value of Simulations

Tracking experiments were carried out with simulated humidity fields, because humidity data are not currently available from existing geosynchronous satellites, and in order to make an assessment of the efficiency and accuracy of the ISODATA technique. The ISODATA computer program determines the motions of various distinct features of a field, and the solution consists of a field of motion vectors. In order to check the solution, a known field of motion vectors must be available with which to compare the program's output. One of the values of a simulation process is that the motion field can be initially specified and is thus known.

2. Generation of Simulated Fields

Actual temperature and humidity profile data were not available for use in this study. Thus, humidity fields were simulated that closely resembled a THIR 6.7 μm photofacsimile image published by Steranka et al. (1973). This image, which is shown in Figure 17, is from the polar orbiting Nimbus 4 satellite. It shows distinctive patterns of the atmospheric water vapor that lie between 500 and 250 mb. It is assumed that this field would be fundamentally similar to one for an isentropic layer.

In this study, fields of clusters were generated to simulate the imagery of Figure 17. This was done by visual inspection of Figure 17, using the cluster-generating language of Hall et al. (1973). In this language, clusters are specified as to their location and size,

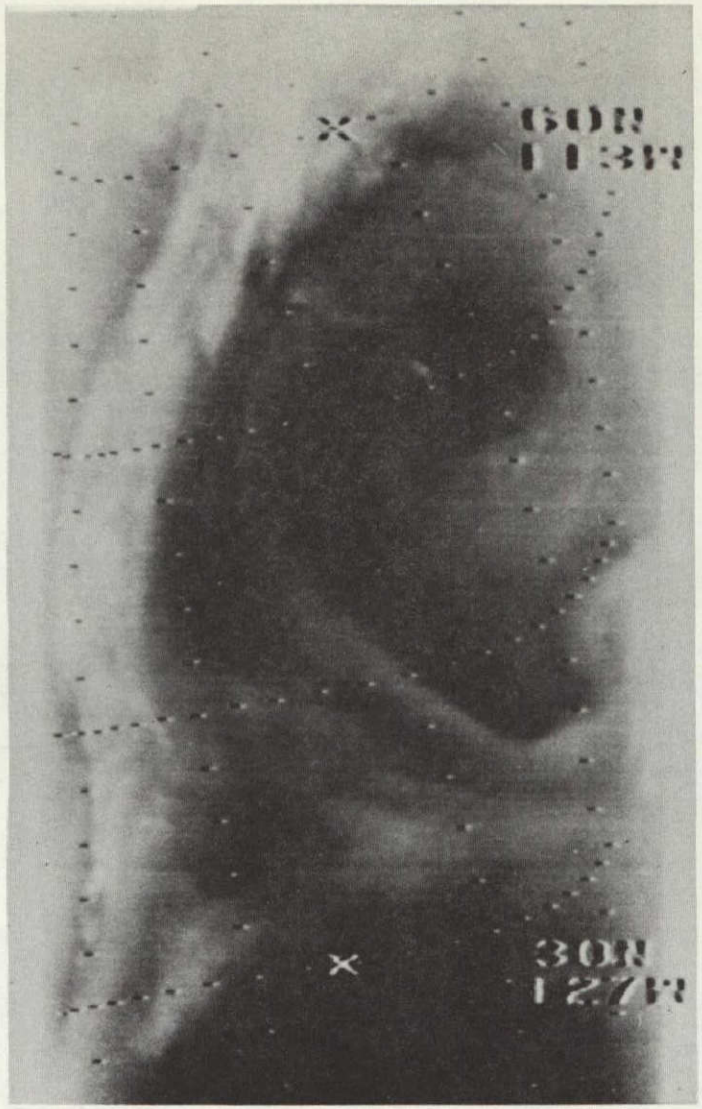

FIGURE 17 NIMBUS 4 THIR 6.7 μm IMAGERY FOR ORBIT 2565, 16 OCTOBER 1970 (TAKEN FROM STERANKA ET AL., 1973)

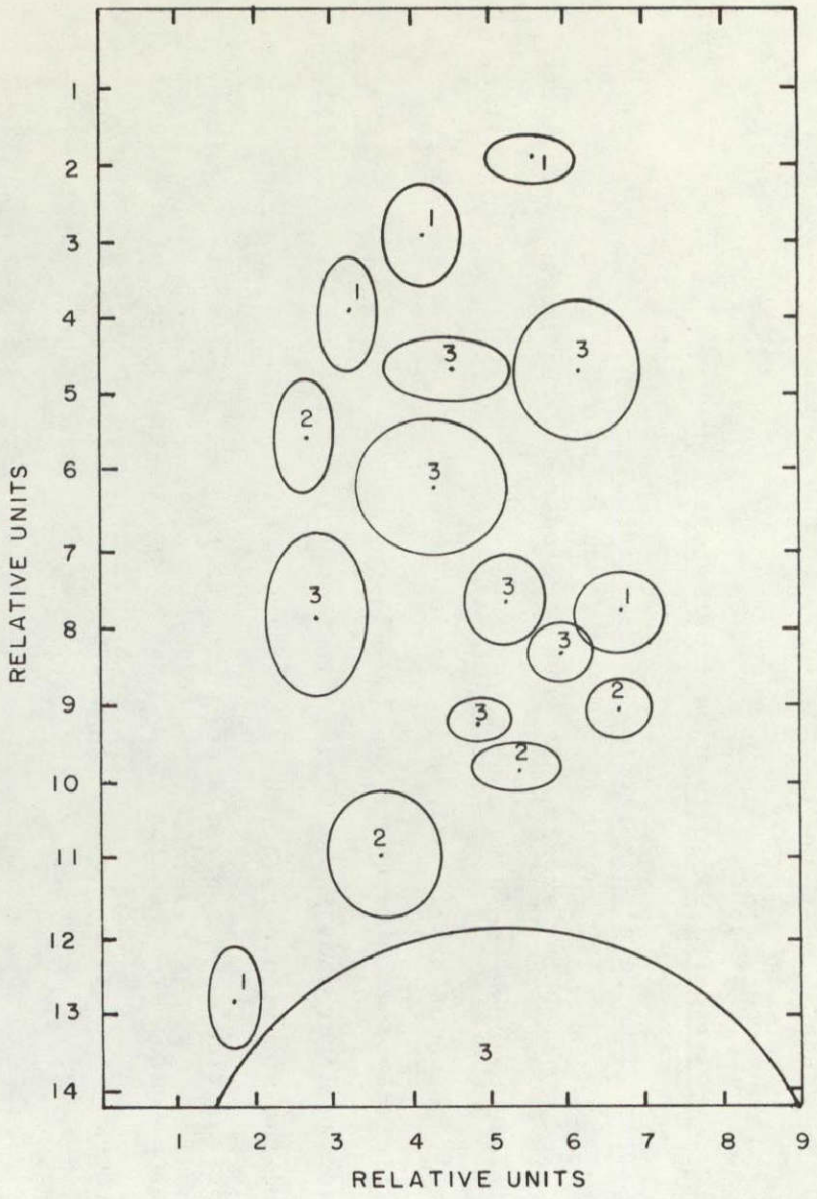

FIGURE 18 ILLUSTRATION SHOWING CLUSTER CENTERS, DEVIATIONS, AND HUMIDITY VALUES (1, 2, 3) THAT WERE USED TO SIMULATE FIGURE 17

within a coordinate system of any number of dimensions. It was decided on an arbitrary basis to track the dry or dark areas of Figure 17, which are represented by the cluster outlines shown in Figure 18. In this study, a coordinate system with three dimensions was used. Two of the dimensions used were the relative units for the abscissa and ordinate shown in Figure 18. For the third dimension, the relative darkness value for the clusters was used; these values are also shown in Figure 18. The clusters are located at different places at successive times according to the specified motion field.

In order to keep the magnitude of the experiment practical and the computer costs within the scope of the project, only a few clusters (17) were generated to simulate Figure 17. More clusters could be used, or even the actual image could be used by making a line-by-line scan of the THIR image in Figure 17. Figure 18 gives simply a simulation of the distorted view of Figure 17. That is, no attempt was made to rectify Figure 17 to give an undistorted image in latitude and longitude. This was not believed to be necessary for this study, and the distortion can be effectively compensated for by specifying cluster motions that take this into account.

The distribution of the data points generated is according to a normal distribution that is obtained by a pseudo-random number generator. The points are spaced with a variance specified by the user. Experimental parameters that are under the control of the program input parameters are the:

- Cluster deviations--If made small, there is no overlapping, and the cluster tracking is relatively easy. If made large, there is overlapping and the cluster tracking is difficult.
- Motion field--Both the directions and magnitudes of the motions are specified for each cluster. In the case simulated, the observed 400-mb winds

provided by Steranka et al. (1973) were used to derive the cluster motions since this was convenient.

- Random number generator--If reset to the same value at the beginning of each time (T_1, T_2, T_3), a maximum consistency occurs between the clusters at each time, making tracking easier. If it is not reset, then statistically identical fields occur, but they are different in detail.

In the case of real data, one must accept the atmosphere as measured. However, in a simulation one can systematically vary each input parameter to cover the entire range.

3. Plots of Simulated Fields

The output from the data generating language appears on the CRT display screen as shown in Figure 19. Three separate times, T_1, T_2, and T_3 were simulated; times T_3 and T_1 are plus and minus two hours from time T_2. The cluster positions at T_1 and T_3 were derived from those specified for T_2 and from the specified cluster motions. The intention of these simulations is to generate data that is reasonably representative of the actual humidity field of Figure 17. These pictures in Figure 19 portray the main features of the humidity field of Figure 17. Each dot on the plots in Figure 19 represents a place where one humidity value is given. At other places on the plots, the humidity values are not specified; in these areas the values are assumed to be thresholded out by computer processing. Three different intensities are displayed, as can be seen by a careful inspection of the brightness of the various clusters of dots. The brighter dots represent the lower humidity regions of Figure 17, while the dark areas represent the higher humidities and clouds.

A cruder but more conveniently generated print-plot version of the data for T_2 is shown in Figure 20. This plot is shown with the

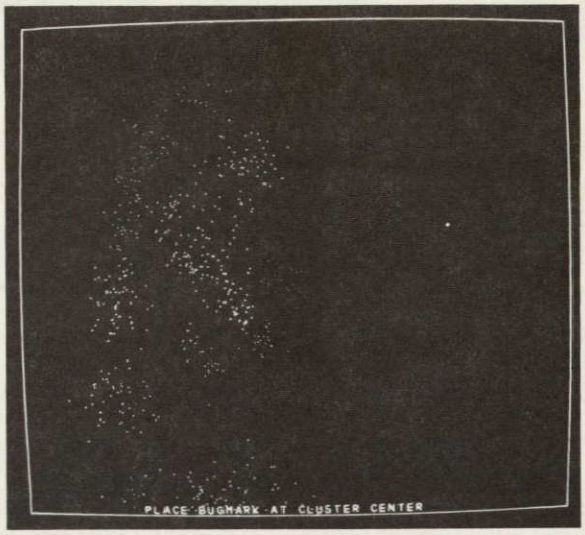

TIME 1 (T_1)

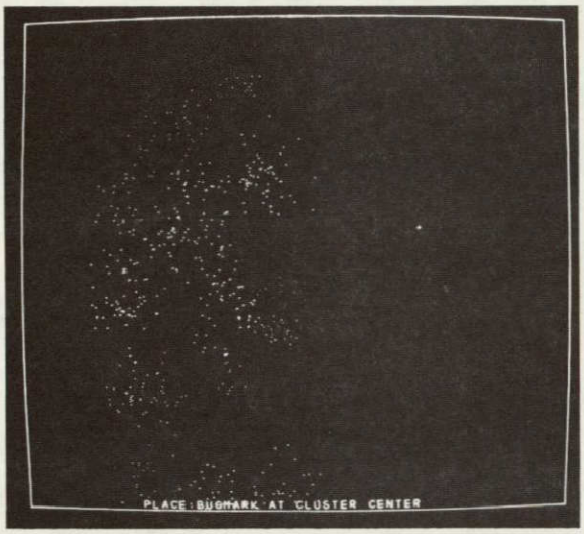

TIME 2 (T_2)

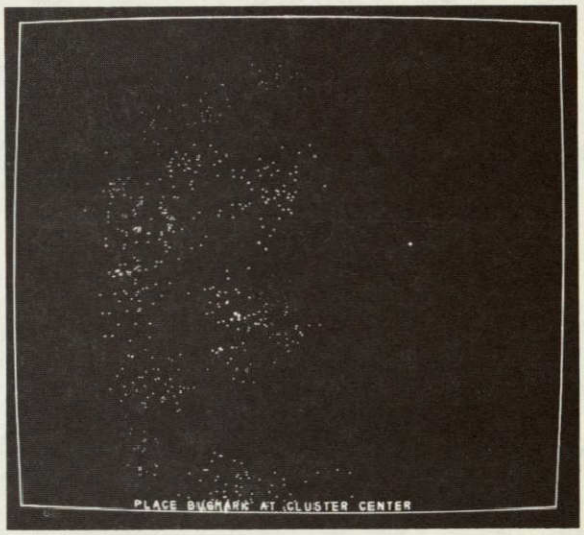

TIME 3 (T_3)

FIGURE 19 CRT DISPLAY OF SIMULATED HUMIDITY FIELDS AT THREE DIFFERENT TIMES (T_1, T_2, AND T_3)

The dots have three levels of brightness with the brighter dots signifying lower humidities; the left side of the time T_2 display is a negative image simulation of Figure 17. The large dot (or + sign) in the right side of all three displays is the bugmark.

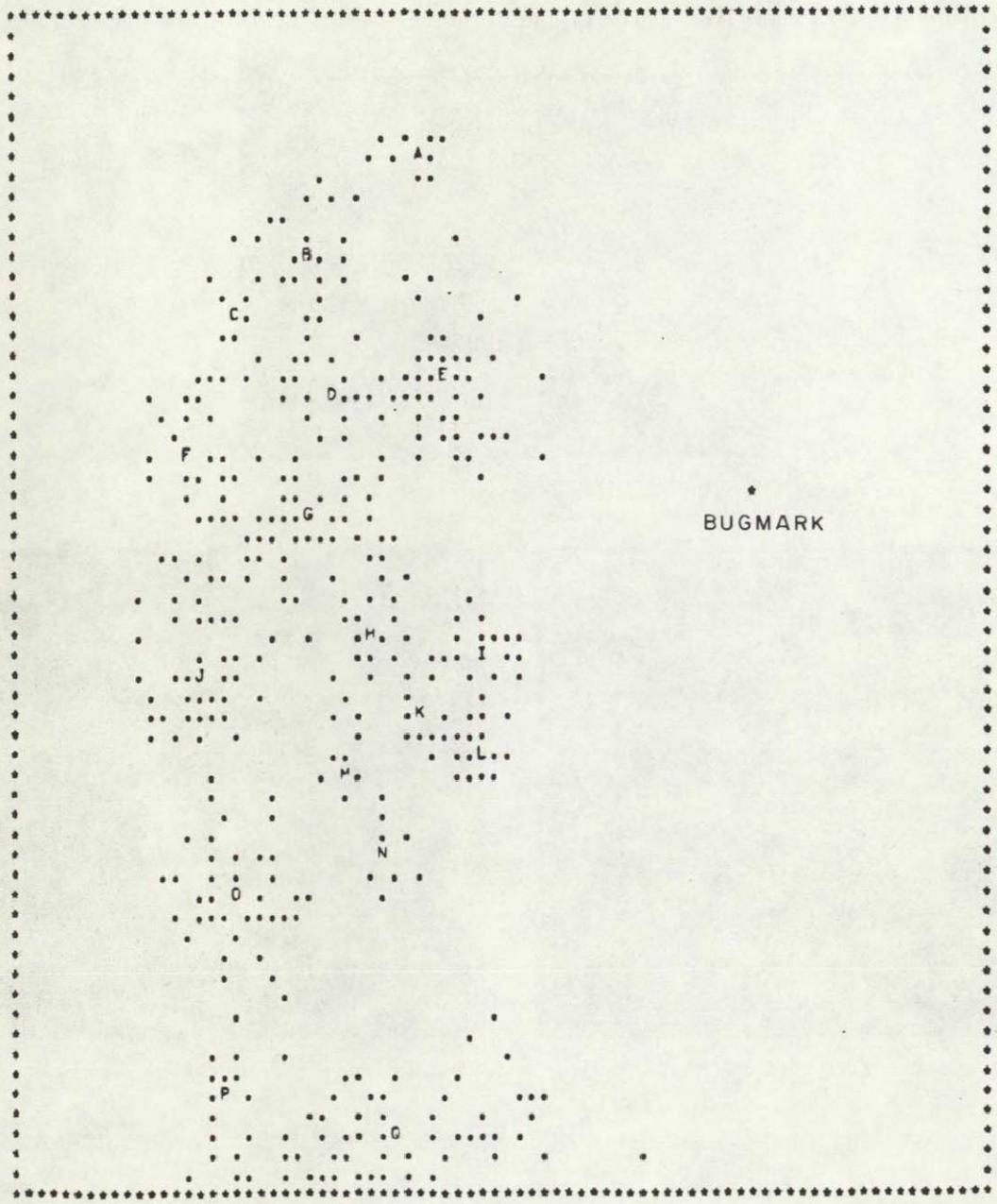

FIGURE 20 PRINT PLOT OF DATA FOR T_2 OF FIGURE 19

This plot does not show the brightness levels.

cluster centers indicated alphabetically. The clusters of data points are statistically generated around a theoretically specified center of values, and would have these centers only if an infinitely large sample were taken. However, the actual centers for the generated clusters were also computed since it was believed to be more realistic to compare the motion program output with the actual centers. Figure 20 shows the actual centers for the T_2 clusters and these differ only slightly from the theoretical centers.

E. Experiments in Automated Tracking of Simulated Humidity Fields

This section of the report describes experiments that were carried out using the PDP 11 and CDC 6400 computer at SRI. The data for the experiments were all simulated as described previously. In all the experiments, the random number generator was set only initially, which means that the fields for the different times (T_1, T_2, T_3) were different in detail, although statistically identical.

1. Low-Cluster Deviations

In one experiment, data fields with low-cluster deviations were generated, because it is a simpler and more logical beginning for testing accuracy. Low-deviation data are more highly clustered, and therefore easier to track uniquely. The data points and cluster centers for this low-deviation field are shown for time T_2 in Figure 21. In this illustration, the cluster centers were located automatically and labeled sequentially, A, B, C, D, ... by the ISODATA program. The locations for cluster centers in this example are seen to be ideally correct, that is in agreement with the generating specifications.

The tracking results are given in Figure 22 and 23, which show the cluster centers as actually generated alongside those tracked by the

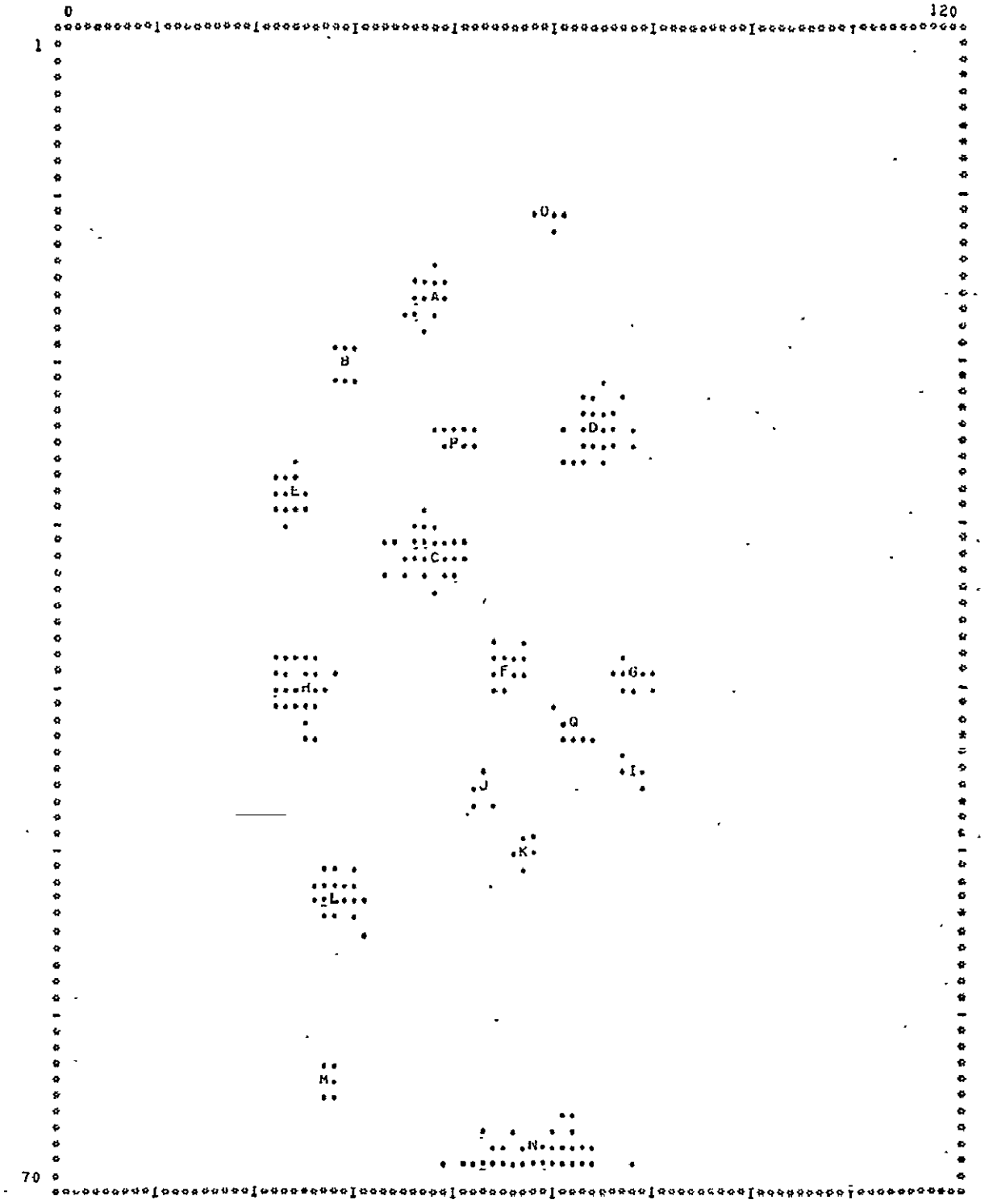

FIGURE 21 DATA POINTS AND CLUSTER CENTERS FOR LOW-DEVIATION FIELD AT TIME T_2

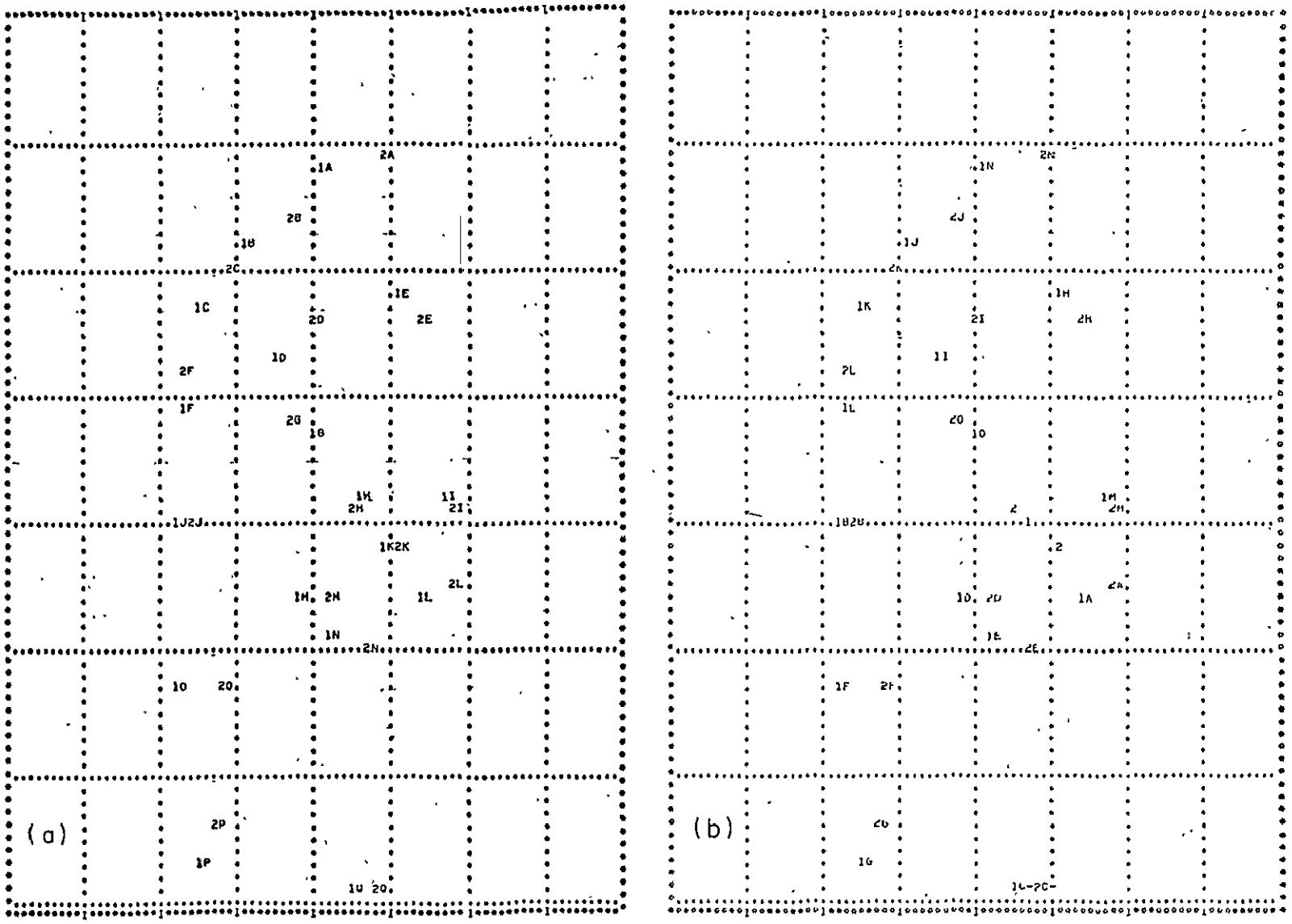

FIGURE 22 TRACKING RESULTS FOR LOW-DEVIATION CLUSTERS USING TIMES T_1 TO T_2

(a) shows the actual cluster displacements and (b) shows the displacements computed by ISODATA (motions go from a 1 to 2 of the same letter).

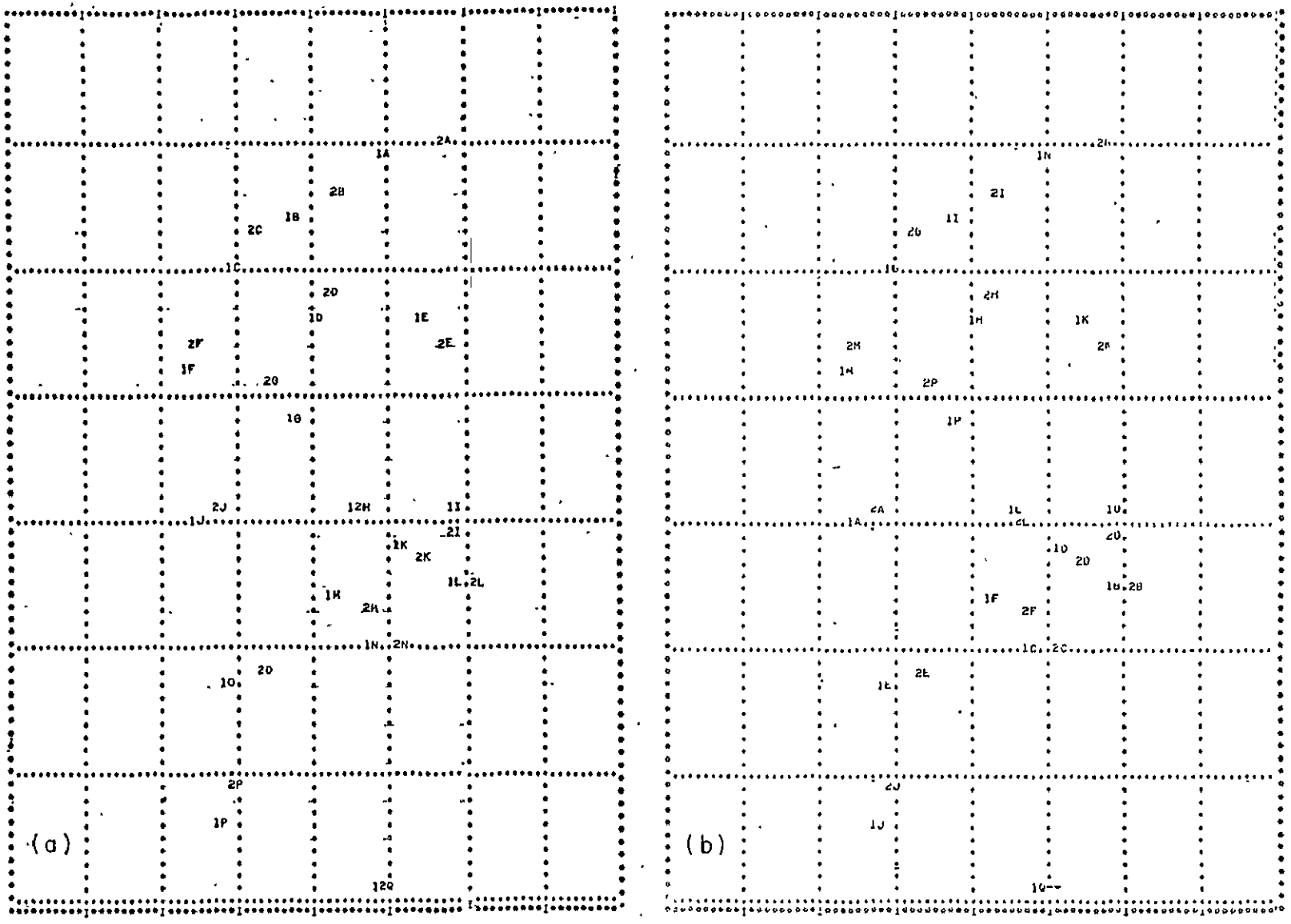

FIGURE 23 TRACKING RESULTS FOR LOW-DEVIATION CLUSTERS USING TIMES T_2 TO T_3

(a) shows the actual cluster displacements and (b) shows the ISODATA displacements.

program between times T_1 and T_2 and between times T_2 and T_3. The sequence numbering in the right-hand plot (ISODATA results) is different from that in the left-hand plot (actual), because of the iterative search process in the ISODATA program. An imperfection shows up in the center of the ISODATA results of Figure 22, corresponding to actual clusters H and K of the left-hand plot. This causes a loss of two motion vectors in the output result; which is not very significant. The information is rejected as being uncertain. This is indicated by giving no alphabetical sequence to these vectors. By changing one parameter in the program--the split/lump threshold--this imperfection would be corrected. In Figure 23, the ISODATA results are entirely correct.

2. High-Cluster Deviations

The overlapping simulated data discussed in this section have deviations that are three times the deviations of the data reported in the preceding section. The generated data as plotted on the line printer were previously shown in Figure 20 for the time T_2. These higher deviations give a better simulation of Figure 17 and are probably more realistic. The theoretical movement of the centers is exactly the same as before. However, because of the small sample of points generated, there are slight differences between theoretical and actual positions of the centers.

The results of processing these data with the ISODATA program are given in Figure 24 for T_1 to T_2, with the actual cluster center displacements alongside for comparison. Again, the alphabetical sequence numbering for the cluster displacements (or vectors) is different because of the iterative search processes used by ISODATA. Actual vector A corresponds to ISODATA vector K, although they are not exactly equivalent, in that the endpoint of K is two columns to the left of the endpoint for A. ISODATA's vector M is quite different from the actual B, although

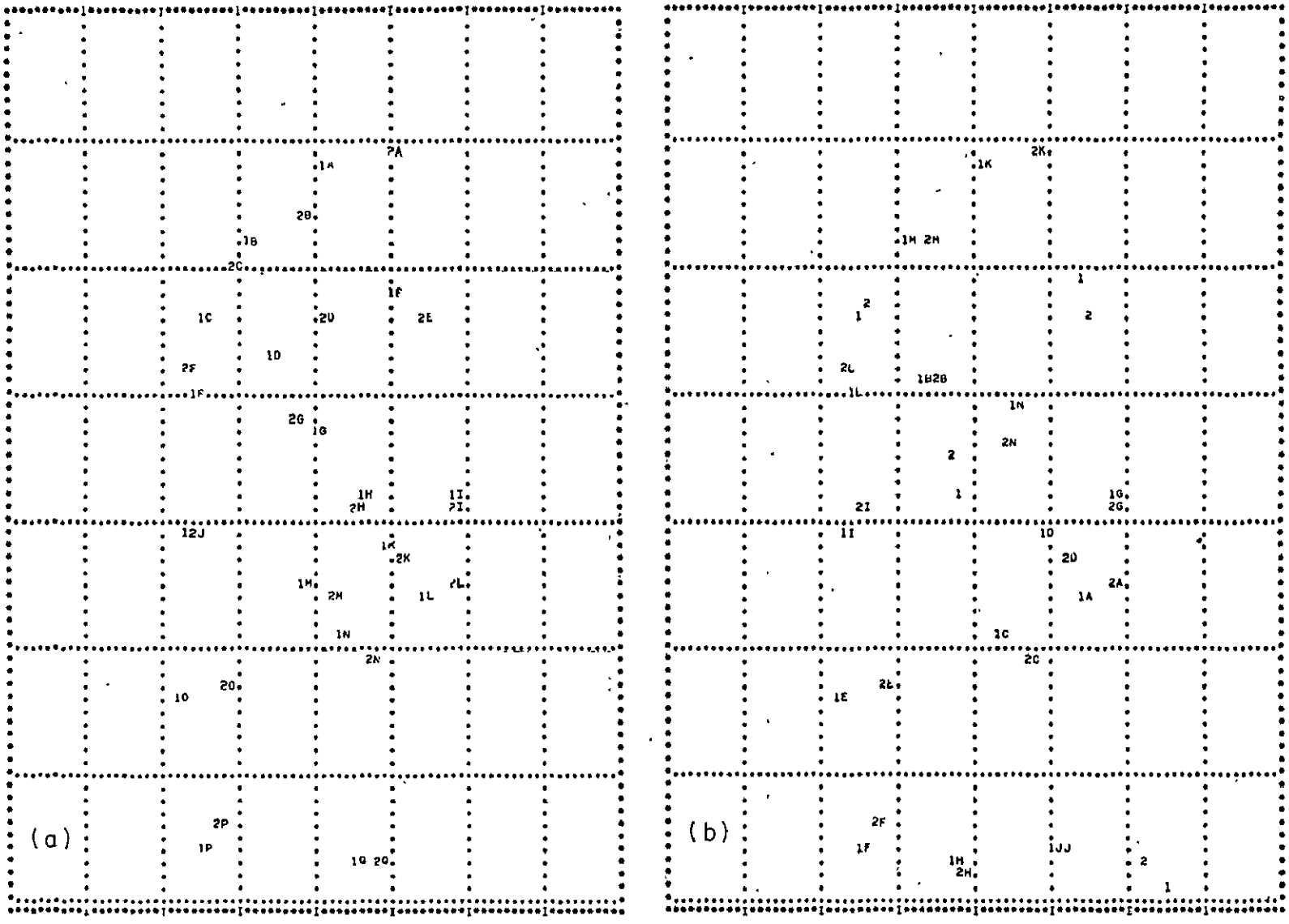

FIGURE 24 TRACKING RESULTS FOR LARGE-DEVIATION CLUSTERS USING TIMES T_1 AND T_2

(a) shows the actual cluster displacements and (b) shows the ISODATA displacements.

they have the same starting point. ISODATA becomes confused with actual vectors C, D, and E, and refuses to assign definite vector labels. However, vector L for ISODATA is in perfect agreement with the actual F, as is ISODATA's A with actual I. Other perfect agreements were obtained with actuals L, N, O, and P, and ISODATA's A, C, E, and F.

Figure 25 gives a similar comparison for the interval T_2 to T_3; these results seem better than for T_1 to T_2. Four different sets of results were obtained by using different initial random numbers--all the results were similar to those of Figures 24 and 25.

An interpolation program was also developed to compare actual and derived vectors since the positions of the vectors can be different. This program also gives an overall rms value for the comparison of all vectors in the frame. The rms error for the motions derived in ISODATA in the high-deviation case was 7m s^{-1}. This is relatively high compared to the average cluster speed of 12m s^{-1}. However, if the few bad results are screened out, then the error is reduced to less than 3m s^{-1}. Automated techniques of screening the data were tested in a previous study (Mancuso and Wolf, 1974).

3. Background Fields

It was found that the addition of a background noise field to otherwise reasonably well-defined humidity centers could cause the original form of ISODATA tracking program to become "confused" in its identification of clusters. This means that ISODATA would find little relationship between two successive pictures, and that the linking of clusters would not be very representative of actual motions. Because of the above difficulties, an improved version of ISODATA was tried which uses a non-Euclidean distance that was first suggested by the Indian statistician

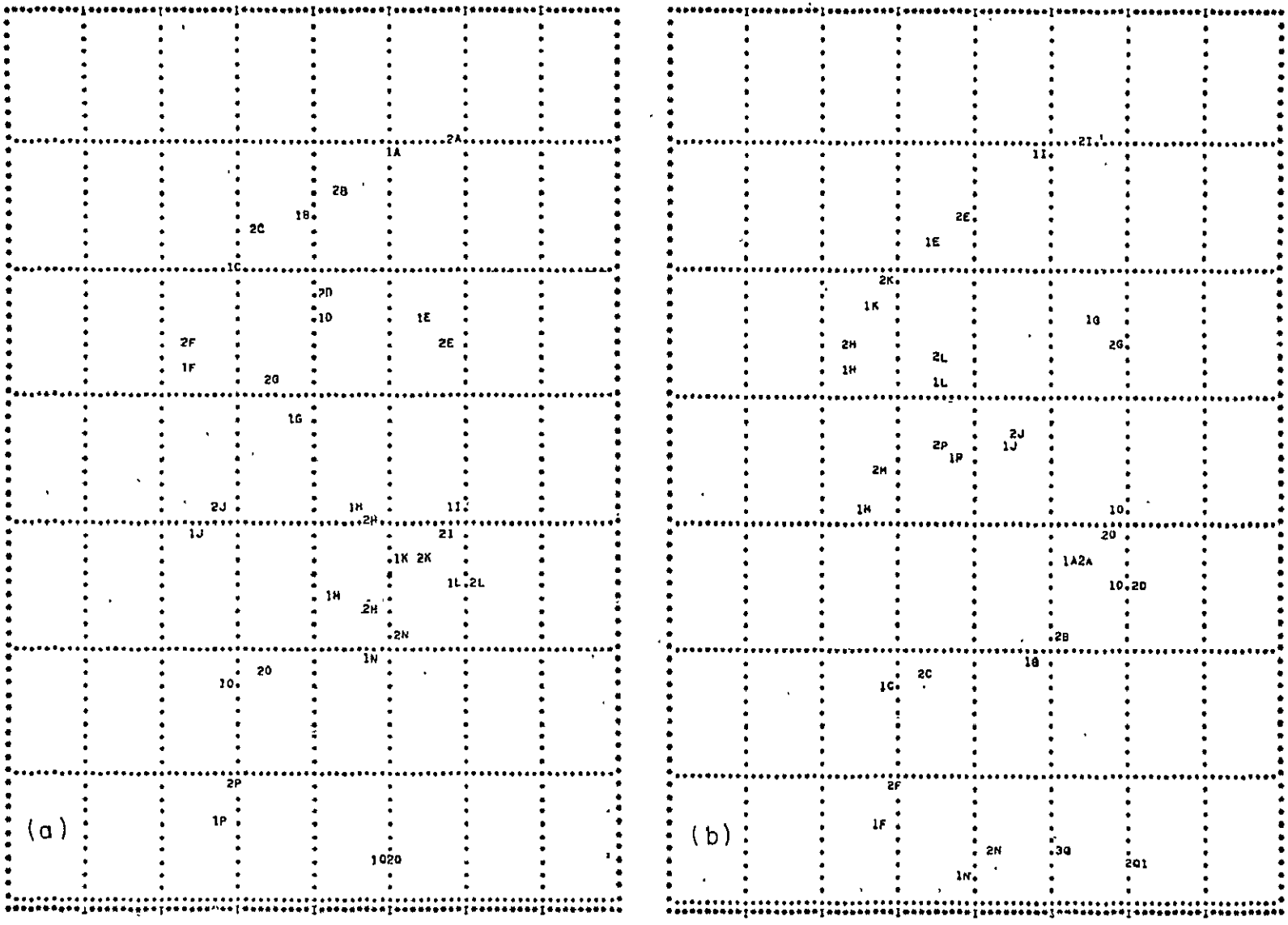

FIGURE 25 TRACKING RESULTS FOR LARGE-DEVIATION CLUSTERS USING TIMES T_2 TO T_3

(a) shows the actual cluster displacements and (b) shows the ISODATA displacements.

Mahalanobis (see Hall et al., 1973). With this approach, more satisfactory clustering results were obtained, although the more sophisticated computation increases the running-time of the program by a factor of about 1.5.

F. Discussion

This study on automated tracking of simulated humidity fields using the SRI ISODATA clustering approach indicates that generally good results can be expected. However, a few bad vectors can occur that produce large rms errors. It would thus be necessary to screen the tracked motions for reasonableness and consistency, using either the human eye or an automated technique. Similar results were obtained in a previous study by Mancuso and Wolf (1974), in which a correlation method was used to track vorticity fields. However, the clustering approach is believed to be more suitable for use with non-rigid entities and it is computationally efficient.

The simulation technique that was used is a fairly simple scheme for generating statistical clusters of points that resemble real humidity fields. It was found to be generally satisfactory for use in verifying, comparing, and improving tracking methods. More complex simulations could also be made, but an increase in cost and time would be involved in both their development and application. Additional tracking studies could be carried out using this simulation technique to determine the:

- Criticalness of data density.
- Optimum values for tracking parameters.
- Number, deviations, and persistency of clusters that produce the most realistic fields (this could be performed by tracking clusters from both simulated and actual data such as the THIR 6.7 μm imagery).
- Accuracy of automated tracking relative to human tracking with a TV electronic console.

IV REFERENCES

Arking, A. A., R. C. Los, and A. Rosenfeld, 1975: An evaluation of Fourier transform techniques for cloud motion estimation. TR-351, Contract NGR-21-002-378, University of Maryland Computer Sicence Center, College Park.

Barnes, S. L., J. H. Henderson, and R. J. Ketchum, 1971: Rawinsonde observation and processing techniques at the National Severe Storms Laboratory. NOAA Tech. Mem., ERL NSSL-53, National Severe Storm Laboratory, Norman, Oklahoma, 246 pp.

Blackmer Jr., R. H., P. A. Davis, R. L. Mancuso, E. J. Wiegman and D. E. Wolf, 1974: Study in the area of satellite meteorology--Vol. 1, Mesoscale weather analysis and prediction. Final Report, Contract DAAD07-73-C-0317, Stanford Research Institute, Menlo Park, California, 136 pp.

Bleck, R., 1973: Numerical forecasting experiments based on the conservation of potential vorticity on isentropic surfaces. J. Appl. Meteor., 12, 737-752.

Brousaides, F. J., 1975: The radiosonde hygristor and low relative humidity measurements. Bull. Amer. Meteor. Soc., 56, 229-233.

Conrath, B. J., R. A. Hanel, V. G. Kunde, and C. Prabhakara, 1970: The infrared interferometer experiment on Nimbus 3. J. Geoph. Phys. Res., 75, 5831-5857.

Danielsen, E. F., 1959: The laminar structure of the atmosphere and its relation to the concept of a tropopause. Arch. Meteor. Geoph. Biokl., 11, 293-332.

Davis, P. A., R. G. Hadfield, and E. J. Wiegman, 1973: Infrared emissivities and upper-tropospheric cloud motions. Final Report, Contract 2-37131, Stanford Research Institute, Menlo Park, California, 55 pp.

Endlich, R. M., D. E. Wolf, D. J. Hall, and A. E. Brain, 1971: Use of a pattern recongnition technique for determining cloud motions from sequences of satellite photographs. J. Appl. Meteor., 10, 104-117.

Endlich, R. M., and R. L. Mancuso, 1972a: Application of some numerical techniques in combining satellite and conventional data in the tropics. J. Meteor. Soc., Japan, 50, 533-541..

Endlich, R. M., R. L. Mancuso, and R. E. Nagle, 1972b: A proposed method for determining winds in cloud-free regions by isentropic analysis of temperature and water vapor profiles. J. Appl. Meteor., 11, 1019-1021.

Endlich, R. M., R. L. Mancuso, and H. Shigeishi, 1972c: Computation of upper tropospheric reference heights from winds for use with vertical temperature profile observations. Mon Wea. Rev., 100, 808-816.

Evans, W. E., 1975: Exploiting the temporal coherence of repetitive satellite imagery. Proc. Symp. Machine Processing Remotely Sensed Data, 3A12-20 (IEEE Catalog No. 75 CH 100g-0-C).

Evans, W. E., and S. M. Serebreny, 1969: Construction of ATS cloud console. Final Report, Contract NAS 5-11652, Stanford Research Institute, Menlo Park, California, 40 pp.

Fuelberg, H. E., 1974: Reduction and error analysis of the AVE-II pilot experiment data. NASA Contract Rep., 120496, National Aeronautics and Space Administration, Marshall Space Flight Center, Alabama, 131 pp.

Fujita, T. T., E. W. Pearl, and W. E. Shenk, 1975: Satellite-tracked cumulus velocities. J. Appl. Meteor., 14, 407-413.

Hall, D. J., R. M. Endlich, D. E. Wolf, and A. E. Brain, 1972: Objective methods for registering landmarks and determining cloud motions from satellite data. IEEE Trans. on Computers, C-21, 768-776.

Hall, D. J., R. O. Duda, D. A. Huffman, and D. E. Wolf, 1973: Development of new pattern recognition methods. ARL 73-0153, Aerospace Research Laboratories, U.S. Air Force, Wright-Patterson Air Force Base, Ohio, 223 pp.

Hall, D. J., F. K. Tomlin, and D. E. Wolf, 1973: Theory and experiments on automatic cloud tracking. Final Report, Contract N62306-71-C-0068, Stanford Research Institute, Menlo Park, California.

Haltiner, G. J., and R. T. Williams, 1975: Some recent advances in numerical weather prediction. Mon. Wea. Rev., 103, 571-590.

Heath, D. F., E. Hilsenrath, A. J. Krueger, W. Nordberg, C. Prabhakara, and J. S. Theon, 1974: Observations of the global structure of the stratosphere and mesophere with sounding rockets and with remote sensing techniques from satellites. Structure and Dynamics of the Upper Atmosphere, F. Verniani (Editor), Developments in Atmospheric Science, 1, Elsevier Scientific Publishing Co., Amsterdam, 131-198.

Hering, W. S., 1965: Ozone measurements for diagnostic studies of atmospheric circulation. AIAA Paper, No. 65-462, AIAA Second Annual Meeting, San Francisco, California, 12 pp. 13 figs.

Kung, E. C., and D. H. McInnis, 1969: Edited NSSL mesoscale upper-air network data in southwestern Oklahoma, 1966 and 1967. Atmospheric General Circulation Tech. Doc., 1, University of Missouri, 7 pp.

Leese, J. A., C. S. Novak, and B. B. Clark, 1971: An automated technique for obtaining cloud motion from geosynchronous satellite data using cross correlation. J. Appl. Meteor., 10, 118-132.

Mancuso, R. L., and D. E. Wolf, 1974: Numerical procedures for analyzing and predicting mesoscale tropic weather patterns. Final Report, Contract DAHC04-71-C-0013, Stanford Research Institute, Menlo Park, California, 54 pp.

Marquardt, D. W., 1963: An algorithm for least-squares esitmation of nonlinear parameters. J. Soc. Indust. Appl. Math., 11, 431-441.

Rossby, C. G., and collaborators, 1973: Isentropic analysis. Bull. Amer. Meteor. Soc., 18, 201-209.

Ruprecht, E., 1975: Diurnal temperature corrections for rawinsonde humidity sensors. Mon. Wea. Rev., 103, 352-355.

Scoggins, J. R., and R. E. Turner, 1974: Data for NASA's AVE-II pilot experiment, Part I - 25 mb sounding data and synoptic charts. NASA Tech. Mem., X-64877, National Aeronautics and Space Administration, Marshall Space Flight Center, Alabama, 530 pp.

Smith, E. A., and D. R. Phillips, 1972: Automated cloud tracking using precisely aligned digital ATS pictures. IEEE Trans. Comput., C-21 715-729.

Smith, W. L., and H. B. Howell, 1971: Vertical distribution of atmospheric water vapor from satellite infrared spectrometer measurements. J. Appl. Meteor., 10, 1026-1034.

Steranka, J., L. J. Allison, and V. V. Salomonson, 1973: Application of Nimbus 4 THIR 6.7 μm observations to regional and global moisture and wind field analyses. J. Appl. Meteor., 12, 386-395.

Thompson, T., 1971: The basic data set project for GARP planning. Bull. Amer. Meteor. Soc., 52, 877-879.

Togstad, W. E., and L. H. Horn, 1974: An application of the satellite indirect sounding technique in describing the hyperbaroclinic zone of a jet streak. J. Appl. Meteor., 13, 264-276.

Wark, D. Q., and H. E. Fleming, 1966: Indirect measurements of atmospheric temperature profiles from satellites, I. Introduction. Mon. Wea. Rev., 94, 351-362.

Wolf, D. E., D. J. Hall, A. R. Toby, and R. G. Hadfield, 1973: Development of an automatic computer system for measuring cloud motion vectors. Final Report, Contract NAS 5-21776, Stanford Research Institute, Menlo Park, California, 91 pp.